

**CZECH TECHNICAL UNIVERSITY IN
PRAGUE**

Faculty of Mechanical Engineering

Department of Automotive, Combustion Engine and
Railway Engineering



MASTER THESIS

**Low-cost particle filter integrity tester for periodic
and roadside vehicle inspections**

August 2021

Submitted by: Yash Patel

Supervisor : doc. Michal Vojtíšek, Ph.D

I. Personal and study details

Student's name: **Patel Yash** Personal ID number: **482807**
Faculty / Institute: **Faculty of Mechanical Engineering**
Department / Institute: **Department of Automotive, Combustion Engine and Railway Engineering**
Study program: **Master of Automotive Engineering**
Branch of study: **Advanced Powertrains**

II. Master's thesis details

Master's thesis title in English:

Low-cost particle filter integrity tester for periodic and roadside vehicle inspections

Master's thesis title in Czech:

Nízkonákladový přístroj pro měření částic při periodických i silničních kontrolách

Guidelines:

The goal of this thesis is to design and present a concept of a low-cost device to test the functionality of a diesel particle filter in a garage, a periodic inspection station, or roadside. The test would supplement the existing smoke opacity testing and would be a low-cost alternative to the non-volatile particle counters recommended by the New Periodic Technical Inspection initiative. The design should use commonly available components with a total cost of less than 100 EUR, not including an ordinary smart phone or a notebook computer. At a minimum, the test should distinguish between a fully functioning and an absent filter on an automobile diesel engine. Being able to do so with an unloaded engine, without free acceleration, would be an added benefit. A proof-of-concept is to be built, tested, and evaluated against a suitable reference measurement on a range of vehicles, assessing, at a minimum, the detection limit and the repeatability of the measurements.

Bibliography / sources:

Burtscher, H. (2005). Physical characterization of particulate emissions from diesel engines: a review. *Journal of Aerosol Science*, 36(7), 896-932. // Burtscher, H., Lutz, T. H., & Mayer, A. (2019). A new periodic technical inspection for particle emissions of vehicles. *Emission Control Science and Technology*, 5(3), 279-287. // Yamada, H. (2019). *Emission Control Science and Technology*, 5(1), 37-44. // Moosmüller, H., et al. (2009). *Journal of Quantitative Spectroscopy and Radiative Transfer*, 110(11), 844-878. // Giechaskiel, B., et al. (2020). *Sensors*, 20(20), 5790.

Name and workplace of master's thesis supervisor:

prof. Michal Vojtíšek, M.S., Ph.D., Department of Automotive, Combustion Engine and Railway Engineering, FME

Name and workplace of second master's thesis supervisor or consultant:

Date of master's thesis assignment: **10.05.2021** Deadline for master's thesis submission: **13.08.2021**

Assignment valid until: _____

prof. Michal Vojtíšek, M.S., Ph.D.
Supervisor's signature

doc. Ing. Oldřich Vitek, Ph.D.
Head of department's signature

prof. Ing. Michael Valášek, DrSc.
Dean's signature

III. Assignment receipt

The student acknowledges that the master's thesis is an individual work. The student must produce his thesis without the assistance of others, with the exception of provided consultations. Within the master's thesis, the author must state the names of consultants and include a list of references.

Date of assignment receipt

Student's signature

I hereby declare that this diploma thesis has been written by me in person. All the information from other works has been acknowledged in the text with the list of references.

In Prague: 13. 08. 2021

Yash Patel

Abstract

The thesis study aims to design and build a prototype of a concept of a low-cost device to test the functionality of a diesel particle filter to whether the vehicle is equipped with a functional DPF or a non-functional DPF. The Number of diesel engines on road is increasing, the diesel engines in recent times are immensely improving their efficiency in reduction of particulate mass but a not higher reduction in particle numbers. Thus, the respective governing bodies are constantly putting out numerous regulations to limit the amount of exhaust particulate produced by a modern-day diesel engine-equipped vehicle to protect human health and the environment. To abide by the evolving regulations, car manufacturers have introduced after-treatment systems in cars. However, the removal and tampering of such after-treatment systems is a common practice by the consumers to avoid extra maintenance costs.

To measure the excess emittance of exhaust particles, a proof-of-concept unit was designed and built, the unit consists of a SHARP dust sensor and commonly available components. The unit was fabricated and tested on three different vehicles. The total cost of the instrument is 40 euro. As the standards instruments exist which usually are expensive and are not accessible to everyone. Therefore, the designed low-cost device can act as a supplementary to existing smoke opacity testing where this device can be used as a primary evaluation device and if further examinations are needed then the vehicle can be sent to the smoke opacity testing.

For the study purpose, once the device was designed which was equipped with a SHARP sensor, certain experiments were conducted under various conditions such as idle, accelerator idle, and free acceleration along with high precision instruments like NanoMet3 and Engine Exhaust Particle Sizer (EEPS). In addition, comparisons were made between the instruments, and repeatability and limit of detection were analyzed. The result showed a good correlation with the high precision instrument at free acceleration and accelerated idle. Finally, it was found that the designed device was capable of distinguishing between a working DPF and an absent DPF. The design can be further developed to attain better results.

Key Words - Low-cost particle filter integrity tester, Sharp dust sensor, Particulate Matter (PM) sensor, Particulate matter (PM), Particulate matter (PM) measurement, Diesel Particulate Filter (DPF), New Periodic Technical Inspection, Arduino.

Acknowledgment

First, I would like to thank my supervisor Doc. Michal Vojtíšek, Ph.D. for giving me this opportunity. His guidance, constant support, and knowledge motivated me throughout my work and helped me achieve my goals. Also, I would like to thank Ing. Martin Pechout, Czech University of Life Science Prague, Faculty of Engineering, Department of Vehicles and Ground Transport for the permission to conduct an experiment and for providing extensive guidance throughout the experiment. Finally, I would also like to thank my beloved parents and my friends for their support and prayers.

The Purchase of components and reference measurements were funded by H2020 project no. 815002 – uCARE – “You can always reduce emissions because you care.”

Yash Patel

Table of Content

| | | |
|-------|---|----|
| 1 | Introduction | 4 |
| 1.1 | Particulate Matter | 5 |
| 1.1.1 | Soot Formation In CI | 5 |
| 1.1.2 | Particle Size & Structure..... | 7 |
| 1.1.3 | Health & Environmental Impact..... | 7 |
| 1.1.4 | Ambient air quality | 8 |
| 1.1.5 | EU Legislation | 11 |
| 1.2 | Reduction of Particulate Matter Emissions..... | 13 |
| 1.2.1 | Diesel Particulate Filter (DPF)..... | 13 |
| 1.2.2 | Disadvantage of DPF | 15 |
| 1.2.3 | Tampering/Removal of DPF..... | 16 |
| 1.2.4 | Prevention of tampering/removing DPF | 16 |
| 1.2.5 | PM Measurement Techniques..... | 17 |
| 1.3 | Detection of High emitters | 19 |
| 2 | Goals of the thesis..... | 21 |
| 3 | Design of proof-of-concept | 22 |
| 3.1 | Choice of sensor | 22 |
| 3.2 | Sharp dust sensor..... | 23 |
| 3.3 | Sharp GP2Y1010AUOF with Arduino | 24 |
| 3.4 | Design of the Low-cost particle filter integrity tester | 27 |
| 3.5 | Cost of Low-cost particle filter integrity tester | 27 |
| 4 | Experimental setup | 28 |
| 4.1 | Validation Instruments | 28 |
| 4.1.1 | NanoMet3 | 28 |
| 4.1.2 | Engine Exhaust Particle Sizer (EEPS)..... | 29 |
| 4.2 | Experiment procedure | 30 |
| 4.3 | Vehicles Used During Experiment..... | 30 |
| 4.4 | Field Setup..... | 31 |
| 4.5 | Time Synchronization Between the Instruments | 32 |
| 4.6 | Particle Mass from EEPS | 33 |
| 4.7 | Pre-processing of Data | 34 |
| 5 | Validation results..... | 35 |
| 5.1 | Particle Size Distribution | 35 |

| | | |
|-------|---|----|
| 5.1.1 | Particle Size Distribution for Vehicle with & without DPF | 35 |
| 5.2 | Gain Factor | 38 |
| 5.3 | Comparison Among Instruments | 39 |
| 5.4 | Repeatability..... | 46 |
| 5.5 | Detection Limit | 48 |
| 6 | Discussion..... | 49 |
| 6.1 | Differentiating between Vehicles with DPF & without DPF..... | 49 |
| 6.2 | Future of Low-cost particle filter integrity tester | 56 |
| 7 | Conclusion | 59 |
| | References..... | 61 |
| | List of Figure..... | 65 |
| | List of Tables | 67 |
| | Appendix..... | 68 |

Nomenclature

| | |
|----------------|---|
| <i>ICE</i> | Internal Combustion Engines |
| PM | Particulate Matter |
| PN | Particle Number |
| DPF | Diesel Particulate Filter |
| HC | Hydrocarbon |
| EU | European Union |
| WHO | World Health Organization |
| AQG | Air Quality Guidelines |
| PTI | Periodic Technical Inspection |
| NPTI | New Periodic Technical Inspection |
| UHC | Unburnt Hydrocarbon |
| DIAS | Diagnostic anti-tampering system |
| HVS | High Volume Sampler |
| LVS | Low Volume Sampler |
| BAM | Beta Attenuation Monitoring |
| FBAR | Film Bulk Acoustic Resonator |
| SMPS | Scanning Mobility Particle Sizer |
| EEPS | Engine Exhaust Particle Sizer |
| CMOS | Complementary Metal-Oxide-Semiconductor |
| <i>CCD</i> | Charge-Coupled Device |
| CAD | Computer Aided Design |
| LED | Light Emitting Diode |
| PEMS | Portable Emissions Measurement System |
| DiSC | Diffusion Size Classifier |
| PMP | Particle Measurement Protocol |
| LOD | Limit of Detection |
| ρ_{eff} | Effective Density |
| σ or SD | Standard Deviation |

1 Introduction

Internal combustion (IC) engines have been used as a source of power production devices by the automotive industry in the transport sector for a long time. IC Engine uses air and fuel mixture to generate power through the combustion process which produces carbon dioxide and water as products of perfect combustion. However, in reality, some intermediate products are produced during the combustion process apart from CO₂ & H₂O. These undesirable intermediate products are collectively known as pollutants and are responsible for air pollution and health issues. These emissions are not exclusively the result of the combustion process, nor do they come only from the tailpipe of the vehicle, rather, they are a result of a combination of the engine design and the fuel properties as well. [1]

Particulate Matter (PM) is one of the major concerns among all the pollutants due to its severe effect on health and the environment. Diesel engines offer higher fuel efficiency but produce more exhaust particulate than conventional gasoline engines. The PM is divided based on their size, particles with diameter of 10 µm and smaller are PM₁₀ and particles with diameter of 2.5 µm and smaller are PM_{2.5}. The prolonged exposure of human lungs to the PM is very dangerous rather than the instantaneous exposure [2]. The decreasing air quality in European nations leads to 379,000 premature deaths according to a survey conducted in 2018, which is an alarming factor for decreasing human life expectancy which is caused by PM with a diameter of 2.5 µm or less [3]. Particulate emissions are controlled by modifying engine design, fuel properties, and by employing exhaust gas after-treatment systems. During this thesis we will discuss more about Particulate emissions.

Some vehicle manufacturers or vehicle owners tamper emission control systems (i.e., Diesel Particulate Filter (DPF)) to increase vehicle performance, increase the fuel economy, decrease the operation costs, and avoid repair costs, Which Increases exhaust emissions in the vehicles, and they are considered as high emitters. Periodic technical inspection (PTI) is leading method to detect high emitters.

1.1 Particulate Matter

Particulate Matter (PM) is a complex component of emission that constitutes a mixture of solid and liquid particles suspended in the air. The physical properties and chemical composition may vary according to the source of emission, location, and several other factors [4]. Figure 1.1-1 [5] shows particle contribution from modern engines is less than 20% for particles smaller than 2.5 μm but the contribution of finer particles (less than 0.1 μm) is around 40%, which is higher in urban areas with intensive traffic. [6]

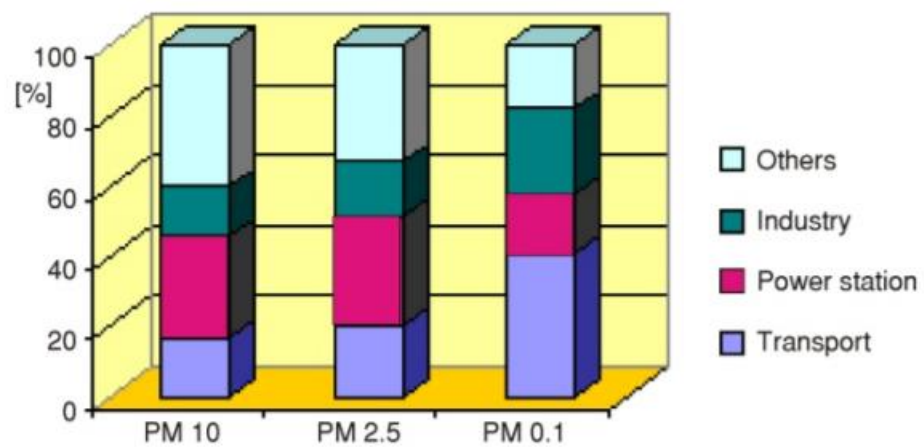


Figure 1.1-1 Contribution of particle matters emission from different sources [5]

1.1.1 Soot Formation In CI

The time scale at which the atomization of fuel occurs in an engine is in order of milliseconds. Such short-time available accompanied with the impingement of fuel on cylinder walls and lower charge temperature, the nucleation breaking of the carbon bonds is not completed. Due to this, the hydrogen manages to escape the HC fuel and leave solid carbon molecules which are known as soot [2] and this process is called nucleation.

The nucleation then proceeds with surface growth, which is the process in which the solid carbon core formed starts to form bigger spheres forming the concentric shells. Hence the surface growth is considered a vital step for the increase in soot mass and volume. The

formation of soot in the surface growth stage is mainly the function of the number of nuclei present at that instance [7].

After the surface growth process, the internal particle collision leads to coagulation in a single spheroid which in turn results in the formation of clusters of solid carbon molecules which is called agglomeration. On one hand, these collision results in a decrease in the number of particles but on the other, this leads to increase of their size which further forms a chain-like structure [7]. Several parameters like engine operating conditions, the performance of injectors, and sampling techniques govern the size of particles [8].

The final stage of particulate matter formation is the absorption and condensation process. The UHC present in the crevices of the compression rings expands in the engine cylinder during the power stroke and remains unburned due as the flame cannot reach them. Also, some UHC are present on the cylinder oil film which does not burn due to flame quenching at cylinder walls. The UHC's get absorbed on the solid carbon surface clusters due to chemical or physical (Van der Waals) forces. Further in the exhaust stroke, condensation occurs when the vapor pressure of UHC exceeds its saturation vapor pressure as the exhaust gases are diluted with air. This completes the formation of PM which can be seen in figure 1.1-2.

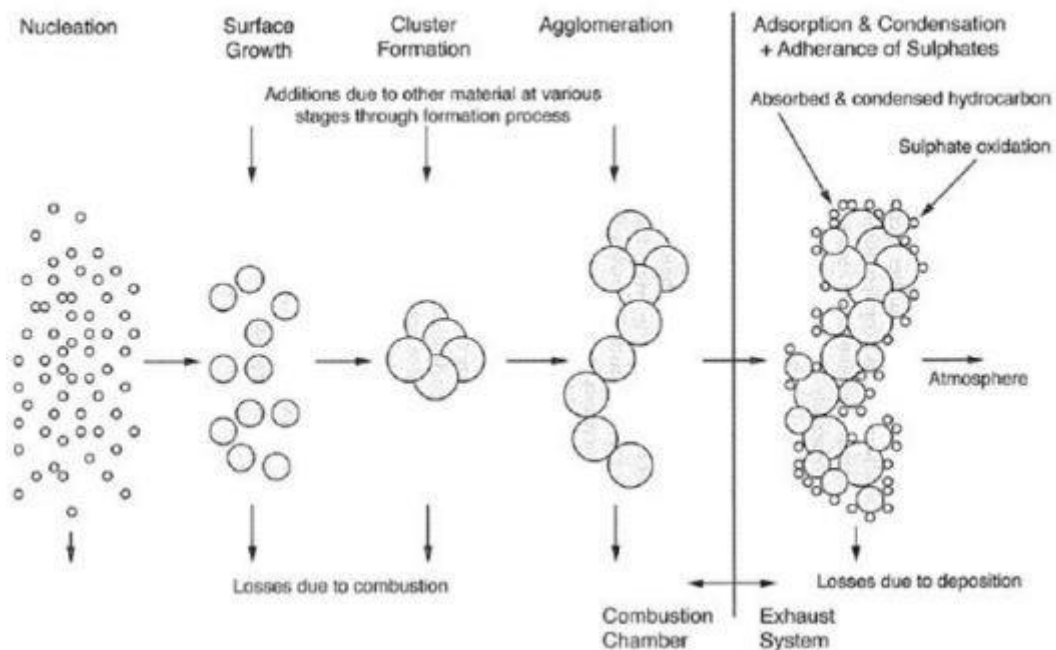


Figure 1.1-2 Stages of soot particle formation [2]

1.1.2 Particle Size & Structure

Particulate matter is not a single pollutant but comprises particles of many different sizes and chemical configurations, from a wide range of natural and anthropogenic sources. The concentration of aerial particles may be measured in numerous different ways. Particulate matter size can be classified into two major categories namely PM_{10} and $PM_{2.5}$ [9]. The PM_{10} category consists of particle size with diameters that are generally $10\ \mu\text{m}$ and smaller whereas the $PM_{2.5}$ fine category consists of particle size with diameters that are generally $2.5\ \mu\text{m}$ and smaller which can be seen in figure 1.1-3 [10].

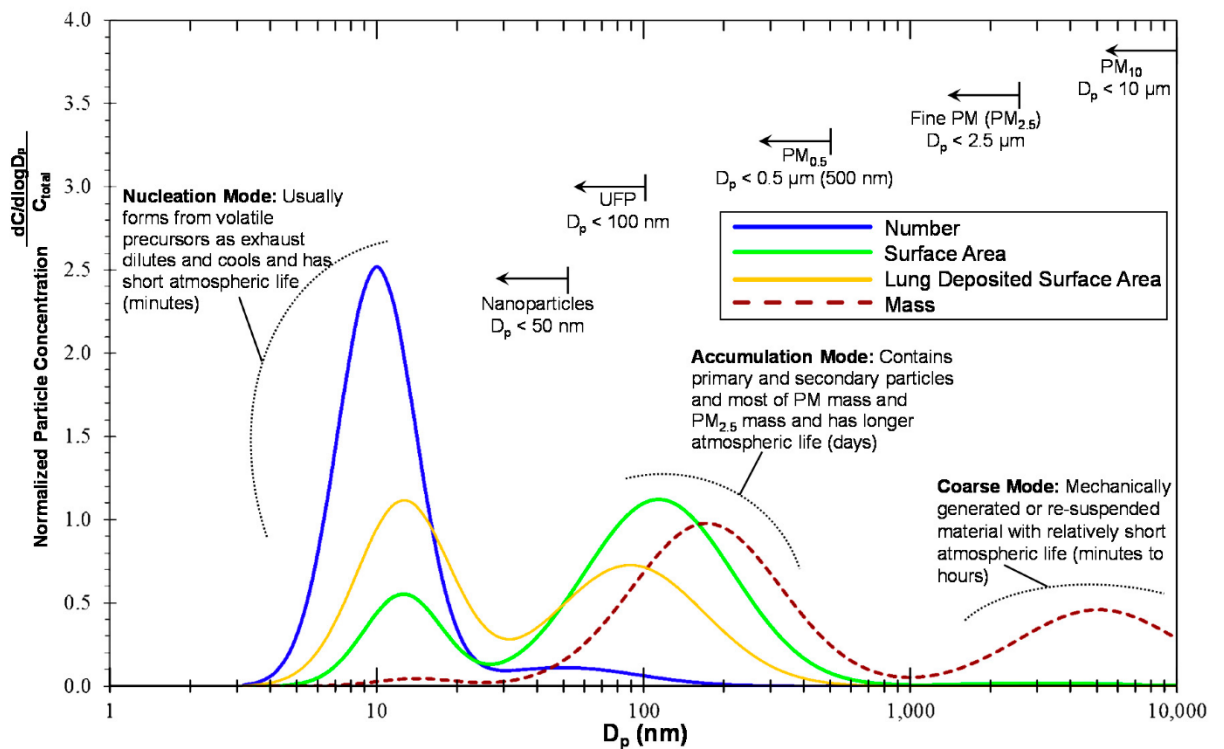


Figure 1.1-3 Particle size distribution (Where, D_p is the particle diameter, UFP are ultrafine particles, and PM stands for particulate matter.) [10]

1.1.3 Health & Environmental Impact

In recent years, the emission of diesel Particulate matter (PM or DPM) has become one of the major health concerns among all diesel emissions. The potential for causing health problems directly depends on particle size. Smaller the particle diameter ($<10\ \mu\text{m}$), the higher the health threats, as smaller particles can get into the lungs and also into the bloodstream. Exposure to such particles can lead following problems:

1. Premature death (approx. 379,000/annum) [3]
2. Nonfatal heart attacks
3. Irregular heartbeat
4. Asthma
5. Decreased lung function

Fine particles (PM_{2.5}) reduces visibility in urban areas and due to their lighter weight can carry over long distances by wind and then settle on ground or water results in contamination of the same (depends on their chemical composition). Soil nutrients are drained by particles that affect the diversity of the ecosystem. Particles are also responsible for acid rain and smog.

1.1.4 Ambient air quality

Governmental agencies and health organizations has set the standards for ambient air quality throughout the world for different harmful pollutants. EU & WHO ambient air quality standards for PM_{2.5} and PM₁₀ is shown in the given Table 1.1-1.

| Pollutant | Averaging period | Legal nature & concentration | Comments |
|-------------------|---|---|--|
| PM ₁₀ | 24 hours | EU limit: 50µg/m ³ | No to be exceeded on more than 35 days per year |
| | | WHO AQG: 50µg/m ³ | 99th percentile (3 days per year) |
| | 1 year | EU limit: 40µg/m ³ | N/A |
| | | WHO AQG: 20µg/m ³ | N/A |
| PM _{2.5} | 24 hours | WHO AQG: 25µg/m ³ | 99th percentile (3 days per year) |
| | | 1 year | EU limit: 25µg/m ³ |
| | EU exposure concentration obligation: 20 µg/m ³ | | Average exposure indicator (AEI)(a) in 2015 (2013-2015 average) |
| | EU national exposure reduction target: 0-20 % reduction in exposure | | AEI (a) in 2020, the percentage reduction depends on the initial AEI |
| | WHO AQG: 10 µg/m ³ | N/A | |

Table 1.1-1 Air quality standards by EU & WHO [3]

Figure 1.1-4 Annual Concentration of PM₁₀ in 2018 shows annual concentrations of PM₁₀ in 2018. The data were received from 3015 stations (116 stations in the Czech Republic) with a minimum coverage of 75%. Total 6% (186 stations) were reported exceeding the annual limit of PM₁₀(40 µg/m³) of all reporting nations including the Czech Republic. The stricter value of WHO AQG for PM₁₀ annual mean (20 µg/m³) was exceeded at 53% (1594 stations) including the Czech Republic.

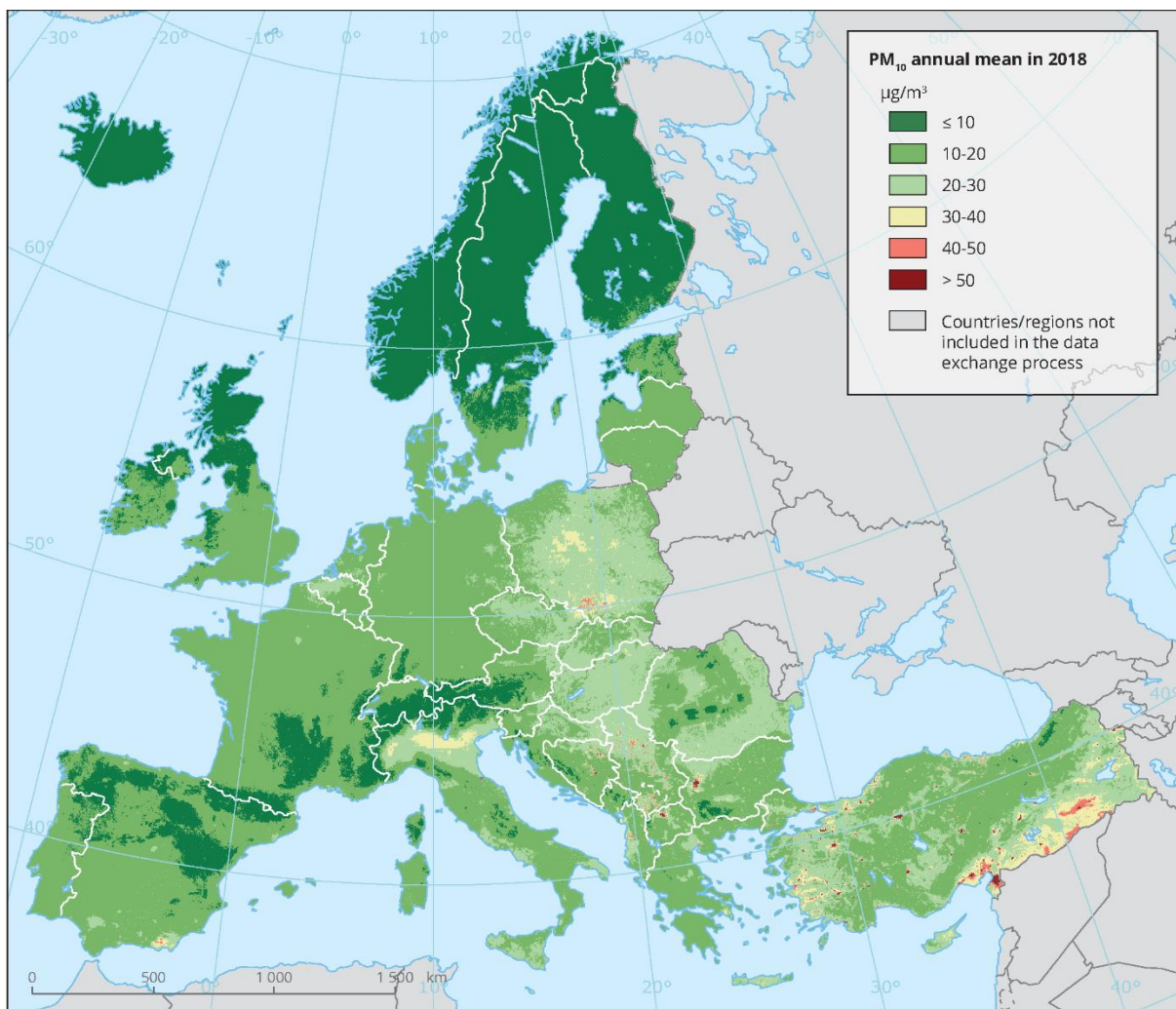
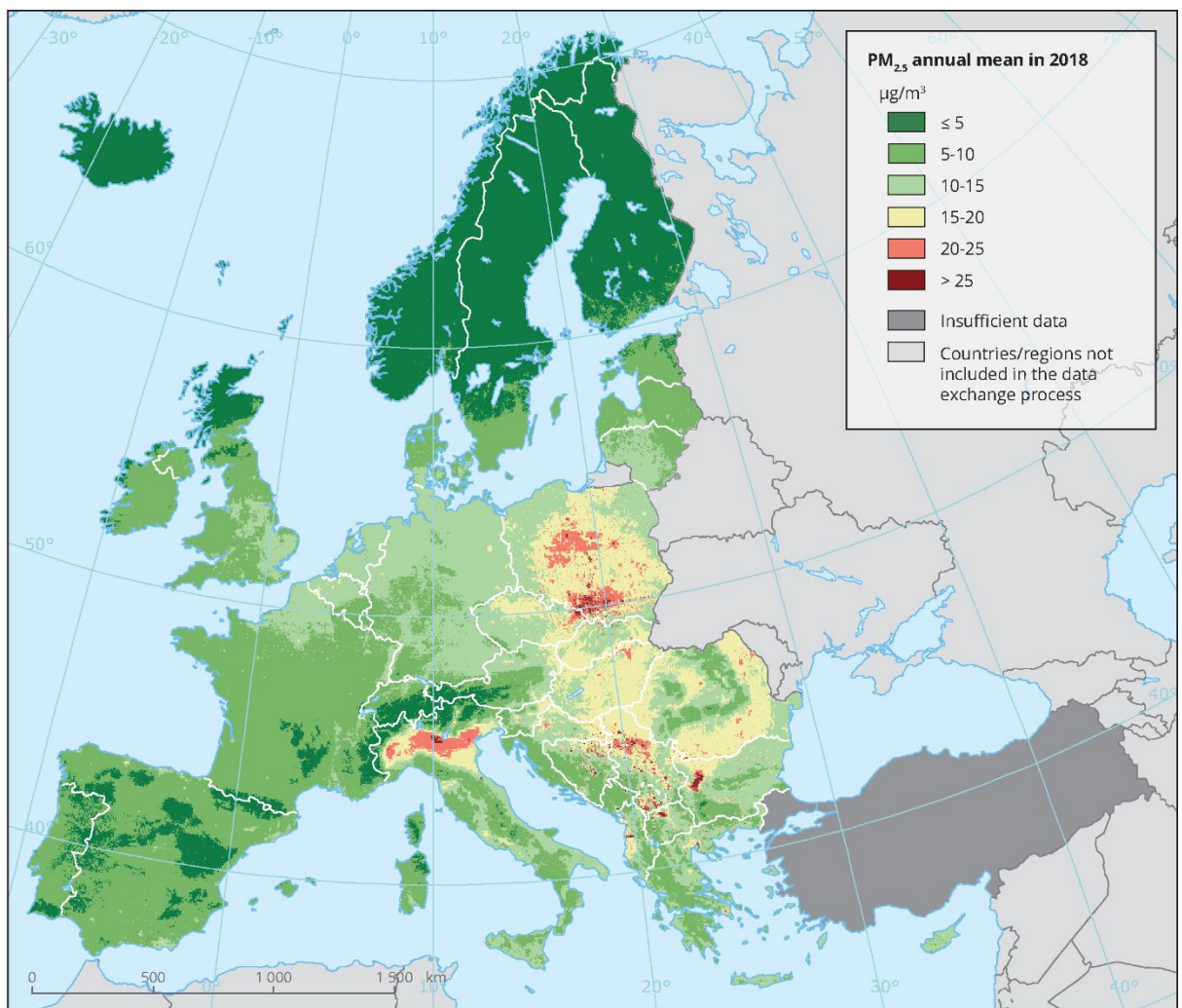


Figure 1.1-4 Annual Concentration of PM₁₀ in 2018 [3]

Figure 1.1-5 shows the annual concentration of PM_{2.5} in 2018. The data were received from 1438 stations (64 stations in the Czech Republic) with a minimum coverage of 75%. In 2018 the PM_{2.5} concentrations were higher than the annual limit (25µg/m³) in six member states including the Czech Republic and two other reporting countries (In total 58 stations). The stricter value of WHO AQG for PM_{2.5} annual mean (10 µg/m³) was exceeded at 70% (1013 stations) including the Czech Republic.

As per the data collected by EEA in the Czech Republic, the annual mean concentrations of PM₁₀ are found to be in-between 12 – 42 µg/m³ whereas the annual mean concentrations of PM_{2.5} are in-between 8 – 38 µg/m³. From the data, it's clear that the Czech Republic is exceeding the mean annual limit for both PM₁₀ & PM_{2.5}.

Note: When it's mentioned that Czech Republic exceeds the limit for both PM₁₀ & PM_{2.5}, it means that some region of the country is exceeding the limit, not the whole country.



Reference data: ©ESRI | ©EuroGeographics

Figure 1.1-5 Annual Concentration of PM_{2.5} In 2018 [3]

1.1.5 EU Legislation

The European Commission has implied certain standards for each vehicle type. Vehicle compliance is determined by running an engine at a standardized test cycle. The vehicle, which is not in compliance with the standardized test, cannot be sold in the European Union. New standards do not apply to vehicles that are already on the roads. From Euro 5 in 2009, Diesel Particulate Filters are used to reduce PM. Table 1.1-2, Table 1.1-3 shows emission standards for diesel passenger cars and diesel light commercial vehicles.

| STAGE | YEAR | CO | HC | HC+NO _x | NO _x | PM | PN |
|-------------|------|------------|----|--------------------|-----------------|------------|----------------------|
| | | g/km | | | | | |
| EURO 1 | 1992 | 2.72(3.16) | - | 0.97(1.13) | - | 0.14(0.18) | - |
| EURO 2, IDI | 1996 | 1.0 | - | 0.7 | - | 0.08 | - |
| EURO 2, DI | 1996 | 1.0 | - | 0.9 | - | 0.10 | - |
| EURO 3 | 2000 | 0.64 | - | 0.56 | 0.50 | 0.05 | - |
| EURO 4 | 2005 | 0.50 | - | 0.30 | 0.25 | 0.025 | - |
| EURO 5a | 2009 | 0.50 | - | 0.23 | 0.18 | 0.005 | - |
| EURO 5b | 2011 | 0.50 | - | 0.23 | 0.18 | 0.005 | 6.0×10^{11} |
| EURO 6 | 2014 | 0.50 | - | 0.17 | 0.08 | 0.005 | 6.0×10^{11} |

Table 1.1-2 emission standards for passenger cars (CI Engine) [11]

| | STAGE | YEAR | CO | HC | HC+NO _x | NO _x | PM | PN | |
|--|---------------|----------------------|------|----|--------------------|-----------------|--------------------|----------------------|------|
| | | | g/km | | | | | | #/km |
| N₁, Class I ≤1305 kg | Euro 1 | 1994.1 | 2.72 | - | 0.97 | - | 0.14 | - | |
| | Euro 2 IDI | 1997.01 | 1 | - | 0.7 | - | 0.08 | - | |
| | Euro 2 DI | 1997.01 ^a | 1 | - | 0.9 | - | 0.1 | - | |
| | Euro 3 | 2000.01 | 0.64 | - | 0.56 | 0.5 | 0.05 | - | |
| | Euro 4 | 2005.01 | 0.5 | - | 0.3 | 0.25 | 0.025 | - | |
| | Euro 5a | 2009.09 ^b | 0.5 | - | 0.23 | 0.18 | 0.005 ^f | - | |
| | Euro 5b | 2011.09 ^d | 0.5 | - | 0.23 | 0.18 | 0.005 ^f | 6.0×10^{11} | |
| N₁, Class II 1305- 1760 kg | Euro 1 | 1994.1 | 5.17 | - | 1.4 | - | 0.19 | - | |
| | Euro 2 IDI | 1998.01 | 1.25 | - | 1 | - | 0.12 | - | |
| | Euro 2 DI | 1998.01 ^a | 1.25 | - | 1.3 | - | 0.14 | - | |
| | Euro 3 | 2001.01 | 0.8 | - | 0.72 | 0.65 | 0.07 | - | |
| | Euro 4 | 2006.01 | 0.63 | - | 0.39 | 0.33 | 0.04 | - | |
| | Euro 5a | 2010.09 ^c | 0.63 | - | 0.295 | 0.235 | 0.005 ^f | - | |

| | | | | | | | | |
|---|----------------------|----------------------|----------------------|------|-------|-------|--------------------|----------------------|
| | Euro 5b | 2011.09 ^d | 0.63 | - | 0.295 | 0.235 | 0.005 ^f | 6.0×10 ¹¹ |
| | Euro 6 | 2015.09 | 0.63 | - | 0.195 | 0.105 | 0.005 ^f | 6.0×10 ¹¹ |
| N₁, Class III >1760 kg | Euro 1 | 1994.1 | 6.9 | - | 1.7 | - | 0.25 | - |
| | Euro 2 IDI | 1998.01 | 1.5 | - | 1.2 | - | 0.17 | - |
| | Euro 2 DI | 1998.01 ^a | 1.5 | - | 1.6 | - | 0.2 | - |
| | Euro 3 | 2001.01 | 0.95 | - | 0.86 | 0.78 | 0.1 | - |
| | Euro 4 | 2006.01 | 0.74 | - | 0.46 | 0.39 | 0.06 | - |
| | Euro 5a | 2010.09 ^c | 0.74 | - | 0.35 | 0.28 | 0.005 ^f | - |
| | Euro 5b | 2011.09 ^d | 0.74 | - | 0.35 | 0.28 | 0.005 ^f | 6.0×10 ¹¹ |
| | Euro 6 | 2015.09 | 0.74 | - | 0.215 | 0.125 | 0.005 ^f | 6.0×10 ¹¹ |
| | N₂ | Euro 5a | 2010.09 ^c | 0.74 | - | 0.35 | 0.28 | 0.005 ^f |
| Euro 5b | | 2011.09 ^d | 0.74 | - | 0.35 | 0.28 | 0.005 ^f | 6.0×10 ¹¹ |
| Euro 6 | | 2015.09 | 0.74 | - | 0.215 | 0.125 | 0.005 ^f | 6.0×10 ¹¹ |

Table 1.1-3 EU emission standards for light commercial vehicles (CI Engine) [11]

1.2 Reduction of Particulate Matter Emissions

The reduction of Particulate matter can be done in the following two ways, first by avoiding the production of particulates or and second by using after-treatment devices – mainly, Diesel Particulate Filter (DPF). Development in engine technology together with improvements in combustion geometry, multi-point fuel injection systems, common rail, etc., are reducing particulates by up to 90%. However, most of the diesel engines are commissioned with Diesel Particulate Filter (DPF) which has a soot trapping efficiency of 95 – 99.9 percent. [12]

1.2.1 Diesel Particulate Filter (DPF)

Over the years, strict emission regulations required diesel engines to become much cleaner. The diesel particulate filter also known as DPF is a filter device fitted to the exhaust system in modern diesel engines. These devices can be fitted before or after the catalytic converter. They require heat to operate correctly. therefore, many DPF are mounted directly after the turbocharger. The design of DPF consists of a honeycomb filter that captures and stores exhaust soot to reduce diesel exhaust emissions. The Figure 1.2-1 shows the basic design of DPF [13]

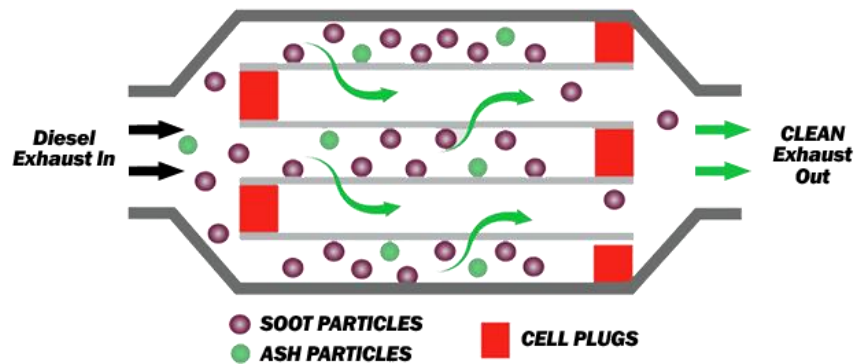


Figure 1.2-1 BASIC CONTRUCTION OF DPF

Due to their finite capacity of trapping soot, the trapped soot periodically has to be emptied or burned off regularly in a process known as regeneration. The regeneration prevents the DPF from blocking up. There are two types of regeneration,

1. Active Regeneration
2. Passive Regeneration

In active regeneration, extra fuel is injected automatically when the filter reaches a predetermined limit to raise the temperature (approx. 600°C) of the exhaust and burn off the stored soot. The passive regeneration occurs when the car is running at speed on a long motorway journey which allows the exhaust temperature to increase to a higher level and cleanly burn off the excess soot in the filter. At the point when the vehicle is no longer operable due to the blockage of DPF, the cleaning of filter or the removal of filter needed to be performed usually at the garages.

Particulate matter emissions are composed of solid particles with adsorbed vapours. The DPF may have reduced or total ineffectiveness in controlling the non-solid fractions of PM, such as SOF or sulphate particulates [12], resulting in an overall efficiency of 70-95%. Therefore, particulate filters tend to increase the formation of nanoparticles through nucleation. In effect, DPFs reduce the numbers of mostly solid agglomeration mode particles, replacing them with mostly liquid nuclei mode nanoparticles as shown in Figure 1.2-2 [12].

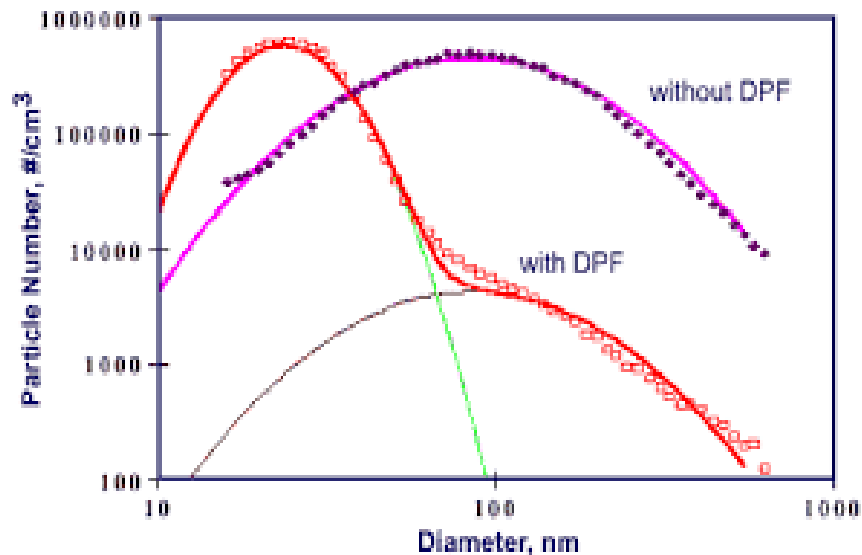


Figure 1.2-2 Particle Size Distribution of Vehicle with & without DPF [12]

1.2.2 Disadvantage of DPF

There are several disadvantages of DPF system which are discussed below.

1. **Reduced fuel economy** – In active regeneration, diesel fuel is introduced into the exhaust stream to increase the temperature which burns off the trapped particulate matter in the filter. This results in significantly reduced fuel efficiency
2. **Reduced reliability, increased downtime** – Filter clogging is one of the major issues which have grown into serious reliability concerns. The DPF should not be clogged, and the regeneration cycle should initiate automatically to periodically clean the filter in ideal conditions, however, filter clogging has become one of the major ongoing problems for many owners which raises a question on the reliability of DPF system.
3. **Safety concerns** – During an active regeneration, the temperature in the exhaust system is raised by 600°C which increases the risk of fire. Trucks equipped with the DPF are advised not to operate in/around tall grass or other environments where is a high risk of starting a fire. Several trucks have been on fire due to malfunction of DPF. so safety also turns out to be one of the concerns as well.
4. **Maintenance/Replacement cost** – If the regeneration doesn't take place then DPF gets clogged which affect the engine operation then force regeneration has to be performed in garages or in worst case the filter needs to be replace which can cost around €1,000-€2,000 [14]

1.2.3 Tampering/Removal of DPF

Although the introduction of Selective Catalytic Reduction(SCR) and the use of diesel exhaust fluid has greatly improved fuel economy [15] & reliability by significantly reducing regeneration cycle frequency, some owners/manufacturers tend to remove or tamper with DPF systems to reduce costs, such as reducing fuel consumption and avoiding the cost and time of maintaining emissions aftertreatment equipment and to increase performances [16].

The tampering of DPF is done by replacing the factory after-treatment system with straight exhaust tubing and by disabling the regeneration system with programming. In practice, it's not that simple to install a section of exhaust tubing as the PCM must be reprogrammed to disable the regeneration system. Without purchasing and installing a complete kit, various troubles may be triggered which will affect the operation of an engine. These tampering devices are easily available in markets and can be purchased through online or in stores and can be installed by Mechanic or technician. Research says that the vehicle with tampered or removed DPF increases particle count by several order of magnitude than vehicles with DPF. DPF [17] [18], these vehicles with very high exhaust emissions are known as High emitters.

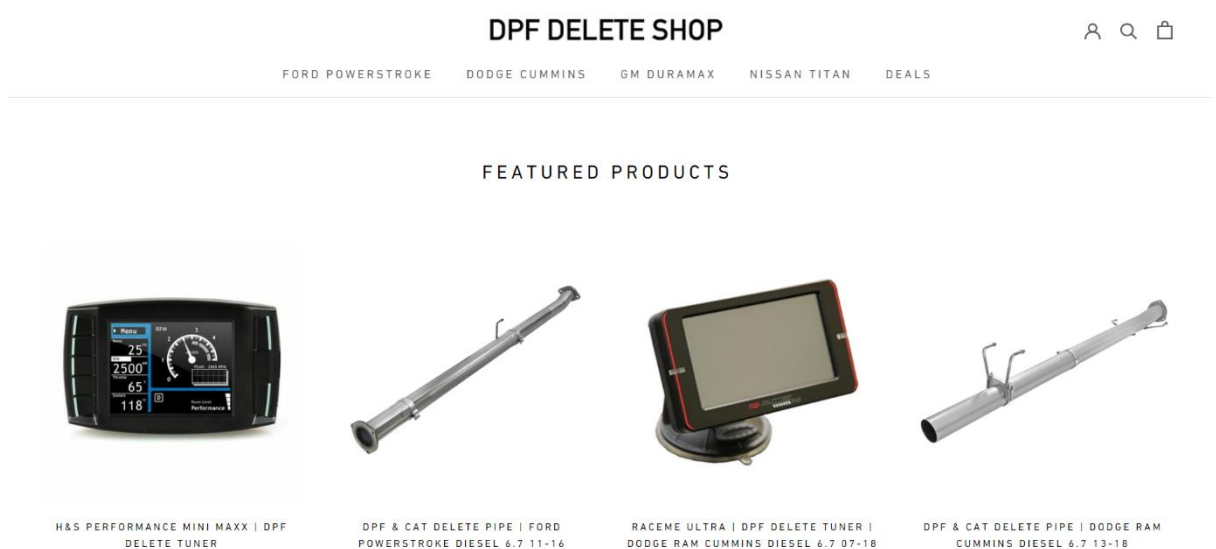


Figure 1.2-3 Tampering devices shop Online [19]

1.2.4 Prevention of tampering/removing DPF

The removal/tampering of DPF can be made difficult by using different approaches and technologies. To harden vehicle emission control systems against tampering EU has launched DIAS (Diagnostic anti-tampering system) project. The objective of the project is to develop techniques to detect and prevent changes to the vehicle's emission hardware or software. In the case of detection, the tampering information would be used to introduce countermeasures, such as the activation of a driver inducement system [20].

In addition, periodical and roadside inspections should be carried out which should include improved visual inspections for hardware modifications, as well as more adequate emission measurement methods [21] furthermore the national laws and regulations should be tightened by prohibiting tampering and by prohibiting the use of tampered vehicles.

1.2.5 PM Measurement Techniques

A variety of measurement techniques have been introduced to comply with current PM emission standards. Each technique has different characteristics. Direct or in-direct measurement can be performed. Table 1.2-1 shows an overview of different PM measurement techniques.

| Method/Class | Type | Reading | Min. Time Resolution | Latency |
|----------------------------|--------|---|----------------------|-----------|
| Gravimetric | direct | Mass | Hours | Day-week |
| β -Attenuation | direct | Mass | Minutes | Minutes |
| TEOM | Direct | Mass | Seconds | Real time |
| FBAR | Direct | Mass | Minutes | Real time |
| NEPHELOMETRY | Direct | Aggregated (particle count, size) | Seconds | Real time |
| OPC/Spectrometry | Direct | particle count, size) | Seconds | Real time |
| Direct Imaging | Direct | particle count, size) | Minutes | Real time |
| Deposition Imaging | Direct | particle count, size) | Minutes | Minutes |
| Aethalometry | Direct | Mass (BC) | Minutes | Real time |
| Capacitive | Direct | particle count, size | Seconds | Real time |
| Photoacoustic Spectrometry | Direct | Absorption | Seconds | Real time |
| Soot Photometer | Direct | Mass (BC) | Seconds | Real time |

Table 1.2-1 Comparison of PM measurement Techniques [22]

The basic principle of these different measurement techniques is discussed below

- Gravimetric – It is a collection method in which particles are deposited on a sampling filter for a given sampling window and later weighted and further analysed. To collect mass sampling over a long-time interval is required. Fine dust is collected by using a High-volume sampler (HVS) and Low volume sampler (LVS). Multiple samples need to be used if PM₁₀ and PM_{2.5} are being monitored.
- β -Attenuation – The Beta Attenuation Monitoring (BAM) method uses the absorption of beta radiation by solids to measure PM. It exploits the very fact that "the absorbed radiation is proportional only to the mass of the filtered material and is independent of

its density, chemical composition, and physical or optical properties" [23]. BAM typically uses a differential measurement approach in which a filter band collects particles from an air stream and the readings from two Geiger counter detectors are compared, one placed upstream and one downstream of the stream of collected air. BAM shows high precision [24] but is not suitable for general ambient use [25]

- TEOM – Tapered Element Oscillating Micro-Balance is a mechanical system that can be used to measure particulate matter. Particles are deposited in a small conical glass tube, which changes the natural frequency of the tube due to an additional mass. From the ratio of mass and frequency, the particle mass can be calculated. TEOM monitors are very sensitive to mechanical noise and large temperature fluctuations.
- FBAR – Film Bulk Acoustic Resonator is a Micro Electrical Mechanical Systems Resonator, which has been proposed for the detection of PM [26]. The particles are forced to deposit on the sensing element by thermophoresis and then the change in resonant frequency is measured.
- Nephelometry – An infrared light from a light-emitting diode or laser is emitted into a measurement chamber from which particles flow. The light is scattered due to the presence of particles in the chamber and detected by a photoreceptor mounted at a fixed angle. A signal is generated that summarises the light scattered by the particles. A mass concentration is determined from the signal. Size discrimination is not possible. Very inexpensive sensors are available on the market.
- OPC/Spectrometry – In laser aerosol spectrometry, a single particle passes through a laser beam so that a particle count can be performed that can be assigned to different bin sizes from the signal pulses. Thus, several size fractions can be measured, e.g. PM10 and PM2.5 [24]. In addition, a Scanning Mobility Particle Sizer (SMPS), a particle size spectrometer, is used to measure the size distribution of the aerosol number by classifying the particles based on their electrical mobility diameter with a Differential Mobility Analyzer (DMA) and counting the particles with a Condensation Particle Counter (CPC).
- Direct Imaging – In direct imaging, an aerosol flows between a light source and a camera. The passing particles obstruct the light and can thus be detected by image analysis, although very high concentrations are required for reliable measurements.
- Deposition Imaging – In deposition imaging [27], the detection is simply done by periodically capturing a high-resolution Complementary Metal-Oxide-Semiconductor (CMOS) or Charge-Coupled Device (CCD) image sensor mounted at an angle of 45°. By illuminating with a uniform light source, the deposited particles obscure individual pixels, which in turn can be counted by comparing the images differentiated in time. Because it relies on gravitational sedimentation, this technique is intended for indoor measurement because it can only measure particles in turbulence-free environments.
- Aethalometry – The sample is drawn through a filter on which the particles collect, with time the filter material becomes darker. Continuous or periodic measurements of the transmission of a laser beam through the collected deposited particles are made until an upper limit for the density is reached. Then the filter material is shifted, and a

new collection area is started. The increase in attenuation of the laser beam over time is proportional to the concentration of BC on the filter.

- Capacitive – In capacitive detection, when a single microparticle enters the electric field between two electrodes, a minute change in capacitance occurs. From the amplitude of the increase in capacitance, the particle diameter can be estimated [28].
- Photoacoustic Spectrometry – In Photoacoustic spectrometry [29], The particles pass through the beam of a modulated laser, i.e., a laser with time-varying intensity, sometimes stronger, sometimes weaker. The irradiated particles absorb the energy, heat up and release the thermal energy into the surrounding air. The heating of the air causes it to expand and generate a sound wave whose frequency corresponds exactly to the modulation frequency of the laser used to excite the particle. The sound wave is then detected by a very sensitive microphone and its amplitude is proportional to the absorption capacity of the particle.
- Soot Photometer – The soot photometer is used to measure black carbon (BC). In this method, particles are illuminated by a powerful laser. The particles absorb the energy of the laser beam, heat up and burn. As they burn, their mass is converted into thermal electromagnetic radiation, called blackbody radiation, which can be measured and is proportional to the mass of the particles [30]

1.3 Detection of High emitters

European legislation requires each Member State to ensure that vehicles registered in its territory are periodically tested by authorized testing bodies. For diesel vehicles, a smoke opacity measurement is carried out during the free acceleration test for the periodic technical inspection (PTI). The opacity limit for modern diesel engines for light commercial vehicles is 0.7m^{-1} [31], which varies by category, year & model of the vehicle.

A smoke opacity meter is an instrument for measuring the optical properties of diesel exhaust that indirectly measures diesel particulate emissions by using physical phenomena such as extinction of the light beam by scattering and absorption. Therefore, opacimeters are used in most diesel engine inspection & maintenance or PTI programs. The diesel smoke opacity test has a poor correlation with vehicle PM/PN emissions [32], resulting in vehicles without DPFs passing the opacity test because the exhaust opacity value is often below the limit. An alternative to the smoke opacity test for performing the PTI is the electronic on-board diagnostic system (EOBD) [31], which may report certain fault codes and is stored in the memory of the electronic control unit (ECU) In the event of a malfunction. OBD system is often tampered with when removing particulate filters and due to the lack of sensors, EOBD systems are unable to monitor and control all emissions. Available vehicles do not yet have PM or PN sensors.

Due to extremely low particulate emissions, a new PTI was needed to identify emission manipulations such as DPF tampering/removal. VERT Association and the Netherlands (Ministry of Infrastructure and Water Management, RDW, TNO, NMI) took an initiative and

introduced an informal NPTI test procedure for diesel particulate filters. The test consists of a PN emission measurement with the vehicle stationary and low idle speed. PN limit for Euro5b/6 vehicles was 250,000 cm⁻³, for earlier stages (Euro 3,4 and 5a) vehicles could have a PN limit of 1,000,000 cm⁻³ [33]. This limit was relaxed to 1,000,000 cm⁻³ for all diesel vehicles under a PTI PN regulation published in 2021. Such a PN measurement is a quick and accurate method of testing the functionality of the DPF.

The Figure 1.3-1 shows the PN emissions of a vehicle with DPF using the NPTI test. It can be clearly seen that the PN value at low idle speed is almost zero and the difference in PN value between ambient air and at low idle speed shows the ability of the PTI PN test to detect vehicles without DPF. It is expected that the European Commission will make a recommendation for the PTI-PN (or NPTI) test procedure in addition to the PTI legislation and consider implementing the PTI-PN test procedure in the Euro 7 type-approval legislation.

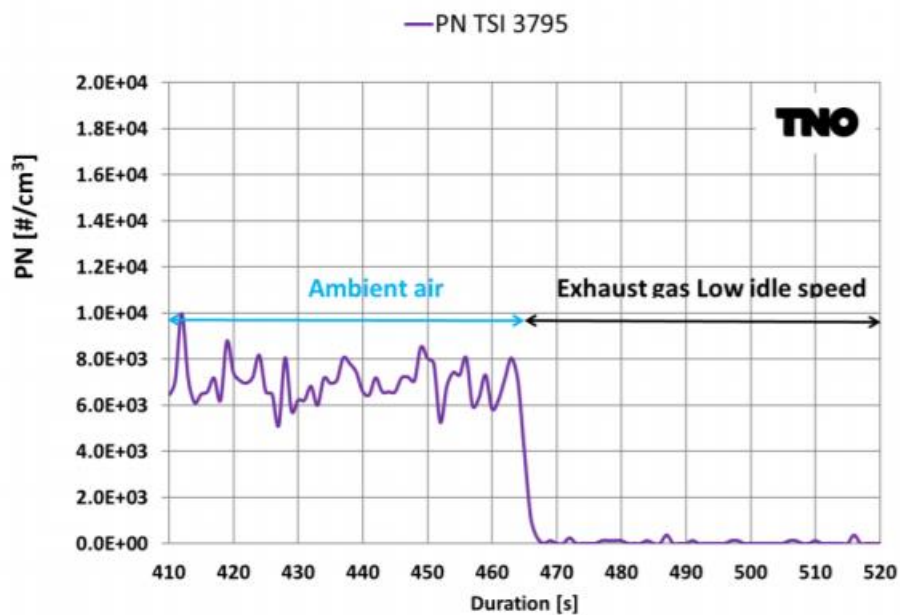


Figure 1.3-1 PN Emission of Vehicle with DPF @ Low idle speed [33]

2 Goals of the thesis

The primary goal of this work is to design and develop a low-cost device capable of distinguishing between a fully functional and a non-functional DPF. The component of the device should be easily available in the market and the cost of the device should not be more than 100 Euro. The various task should be performed are

- To select a sensor to measure PM.
- Design & fabricate proof-of-concept of a low-cost device.
- To conduct an experiment on the vehicles with DPF and without DPF.
- To compare the newly developed low-cost device with reference instruments used in a parallel.
- Validation and calibration of the low-cost device and to find the detection limit of device.
- Repeatability and test-to-test variance by collecting data from vehicles multiple times and finding out the uncertainty of low-cost devices.

3 Design of proof-of-concept

3.1 Choice of sensor

From the previous section (1.2.5), we can conclude that light scattering may be the most suitable technology for a portable, low-cost PM measurement. This section focuses on the selection of the appropriate sensor. There are certain criteria into which the sensor should fall, they are,

- Compact – The sensor should be small in size and easily attached or mounted to any component
- Inexpensive – Since we are looking for a cost-effective device, the sensor should be affordable and easily available
- Usable – The sensor should require very little maintenance as possible which is the key to acceptance
- Accurate – When measured values are subject to high noise or uncertainty, the value of the data decreases. Of course, accuracy requirements depend on the specific use case, and trade-offs between price and data quality are inevitable. At the very least, the measured values must provide added value to the overall system in which they are used.
- Responsive – Low latency (Timeliness) of data is desirable.

Nowadays, many companies offer small and inexpensive light scattering sensors, but very few are capable of measuring particulate matter mass concentration. A laboratory investigation [34] was conducted to compare three inexpensive sensors, namely Shinyei PPD42NS [35], Samyoung DSM501A [36] and Sharp GP2Y1010AU0F [37], with a suitable reference. Several parameters were investigated, which are,

1. Linearity of response
2. Precision of measurement
3. Limit of detection
4. Concentration resolution
5. Response time
6. Interference equivalents
7. Relative humidity

In the experiments, Sharp GP2Y1010AU0F sensor shows moderately good performance in most parameters [34]. Through the depth investigation and comparison among other low-cost light scattering device, Sharp GP2Y1010AU0F looks promising. Therefore, Sharp GP2Y1010AU0F sensor is used for the further experiments.

3.2 Sharp dust sensor

The Sharp GP2Y1010AU0F sensor is a PM dust sensor typically designed for air purifiers. The Sharp dust sensor operates on the principle of light scattering and has an analog output. Figure 3.2-1 shows basic construction along with the principle of the sensor. In the rectangular housing of the sensor, which has a dust through-hole on both sides, a photodetector and an LED emitter face each other obliquely. Dust-laden air flows into the sensor chamber and causes light from the LED emitter to scatter toward the photodetector. The more dust in the air inside the sensor chamber, the greater the intensity of the scattered light. The dust sensor outputs a voltage value that varies according to the intensity of the scattered light, which in turn corresponds to the dust content of the air.

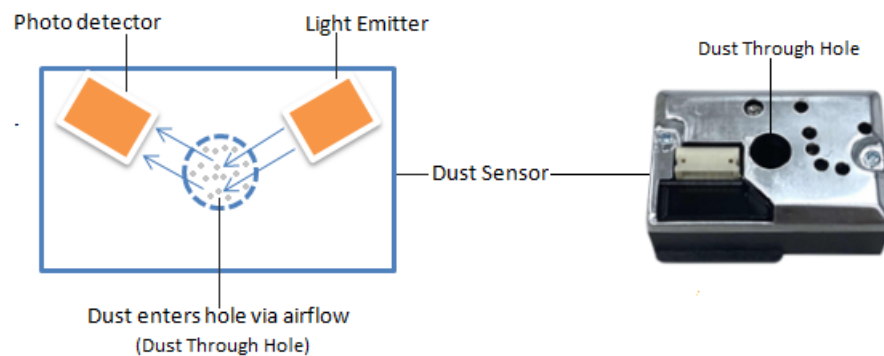


Figure 3.2-1 Sharp GP2Y1010AU0F Sensor Working Principle [38]

The Internal working schematic is shown in Figure 3.2-2,

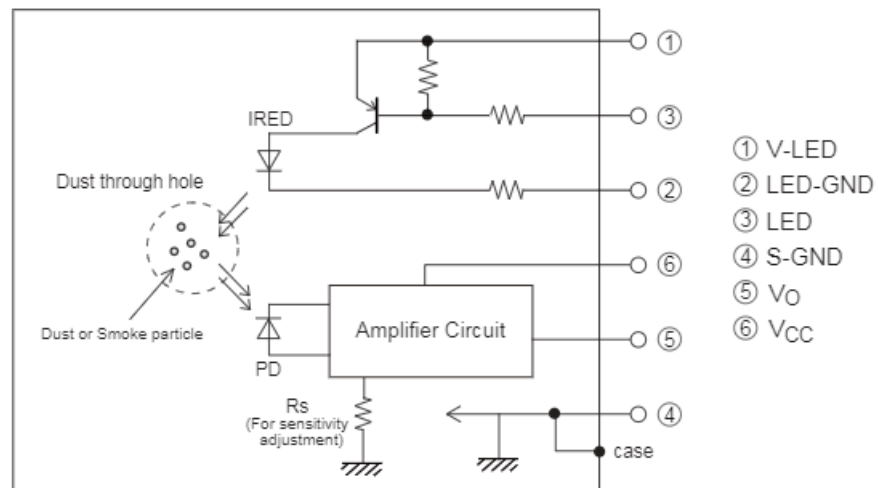


Figure 3.2-2 Internal working Schematic Sharp GP2Y1010AU0F [41]

The Sharp GP2Y1010AUOF measures total mass concentration, which includes concentrations of 1 μm , 2.5 μm , 10 μm , etc. It should be noted that the sensor does not distinguish between PM2.5 & PM10. But when the measured mass concentrations are very high, such as smoking, most of the measured concentration is due to PM2.5. The sensor can distinguish between normal dust and smoke because smoke is high density with small particles and is diffuse, while dust is large and low density and periodically enters the detection area, so one can distinguish between dust and smoke by analysing the output signal. Table 3.2-1 Shows specification of Sharp GP2Y1010AUOF.

| Specification Parameter | GP2Y1010AUOF |
|----------------------------|---|
| Light emitting element | LED |
| Min. detectable dust size | 0.5 μm |
| Dust density sensing range | 0 to 600 $\mu\text{g}/\text{m}^3$ |
| Sensing time | < 1 second |
| Sensitivity / Accuracy | 0.5V \pm 0.15V per 100 $\mu\text{g}/\text{m}^3$ change Accuracy \pm 30% |
| Output interface | Analog |

Table 3.2-1 Specification of Sharp GP2Y1010AUOF [38]

3.3 Sharp GP2Y1010AUOF with Arduino

Arduino is an open-source platform that provides easy use of hardware & software. It consists of both a physical programmable circuit board known as a microcontroller and IDE (Integrated Development Environment) running on a computer used to write and upload a code to a board. Arduino simplifies the process of working with microcontrollers. There are several reasons to choose Arduino over other physical computer microcontroller platforms such as Arduino is inexpensive, runs on most operating systems, is user-friendly, open source with expandable software & hardware. [39]

In addition, Sharp GP2Y1010AUOF is compatible with Arduino. There are several Arduino boards available in the market varies in the specification, here we are using Arduino Uno, which meets our requirement. The sensor requires a resistor (150 Ohm) and a capacitor (220 μF) to turn the sensor LED pulse on and off instead of running it continuously, as it should help to offset the background.

Along with Arduino Uno, we need a breadboard to build the circuits. Breadboards are great units for making temporary circuits and requires no soldering. Figure 3.3-1 the example of a system connection and Figure 3.3-2 shows a supplementary circuit that is used during the experiments.

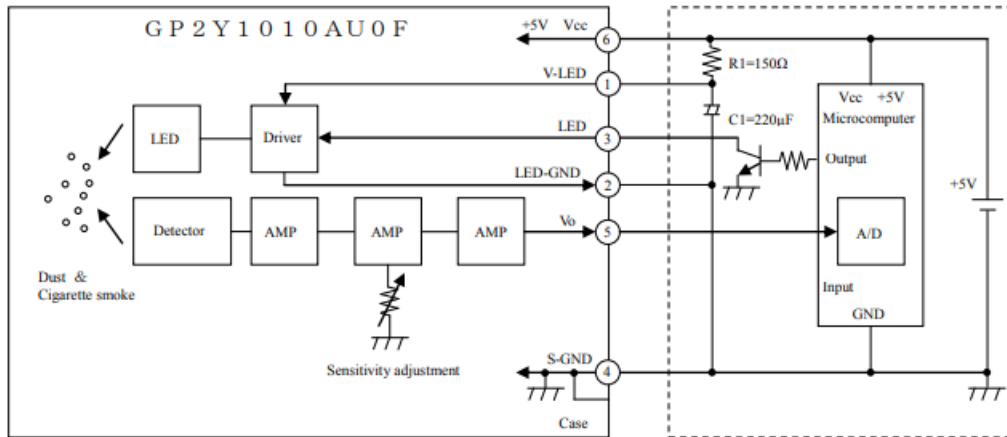


Figure 3.3-1 System Connection [40]

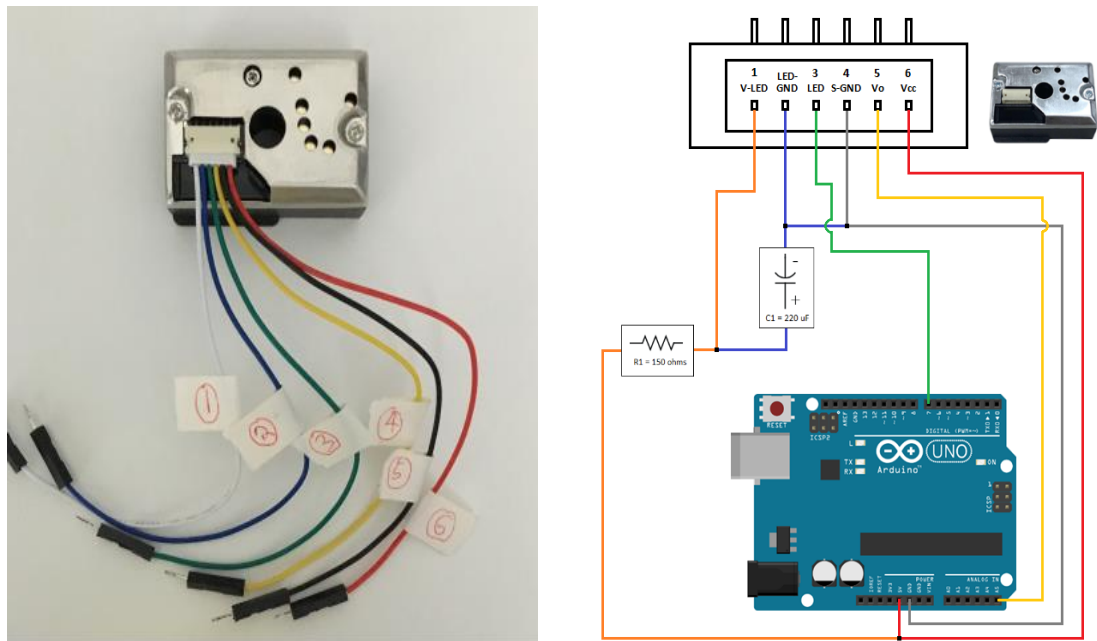


Figure 3.3-2 Complete Circuit [47]

The calculating equation for mass concentration is shown below,

$$\text{Mass Concentration} \left(\frac{\mu\text{g}}{\text{m}^3} \right) = \left(\frac{\Delta V}{K} \right) \times 100$$

Where $\Delta V = V_{OUT} - V_{OC}$

V_{OUT} : Output at no concentration (Typically = 0.9) [41]

V_{OC} : Output at measuring concentration

K : Sensitivity (Typically = 0.5) [41]

The shown equation is used in programming and Figure 3.3-3 shows output from the sensor as displayed on the Arduino serial monitor. Figure 3.3-4 shows sensor characteristic. From the figure it is seen that concentration increases linearly with the output voltage and then at maximum voltage gets constant. In addition, it is seen that even in clean environment the sensor shows non-zero voltage which can be used for the offset correction.



Figure 3.3-3 Arduino Serial Monitor Output

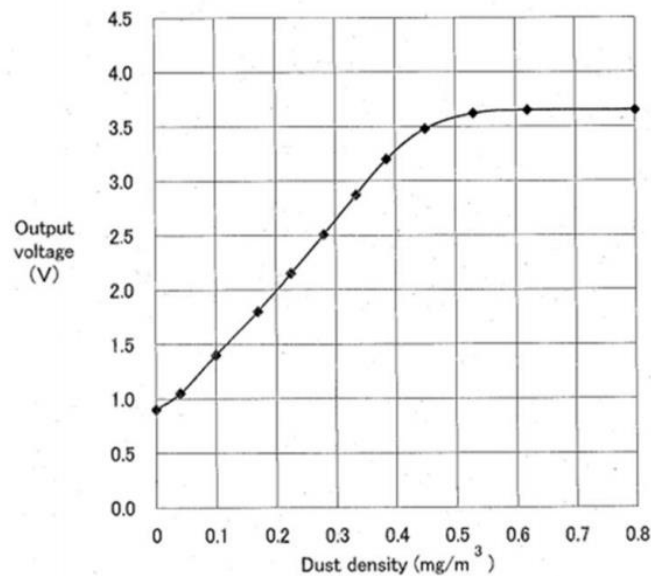


Figure 3.3-4 GP2Y1010AUOF Characteristics [40]

3.4 Design of the Low-cost particle filter integrity tester

Figure 3.4-1 Shows a 3D CAD model of the low-cost device. The sensor is mounted inside a cylindrical insulated pipe. One end of the pipe consists of a sampling pipe of 80 mm rigidly fixed to the pipe housing and concentric with the sensor's opening hole. The other end of the pipe consists of a 50mm diameter fan that runs on a 12v battery. The fan is used to supply airflow to the sensor which will allow the sensor to react quicker. Sensor is connected to the Arduino and the breadboard externally with Suitable wiring. A small hole is drilled into the pipe housing to make a way for the sensor's connector cable.

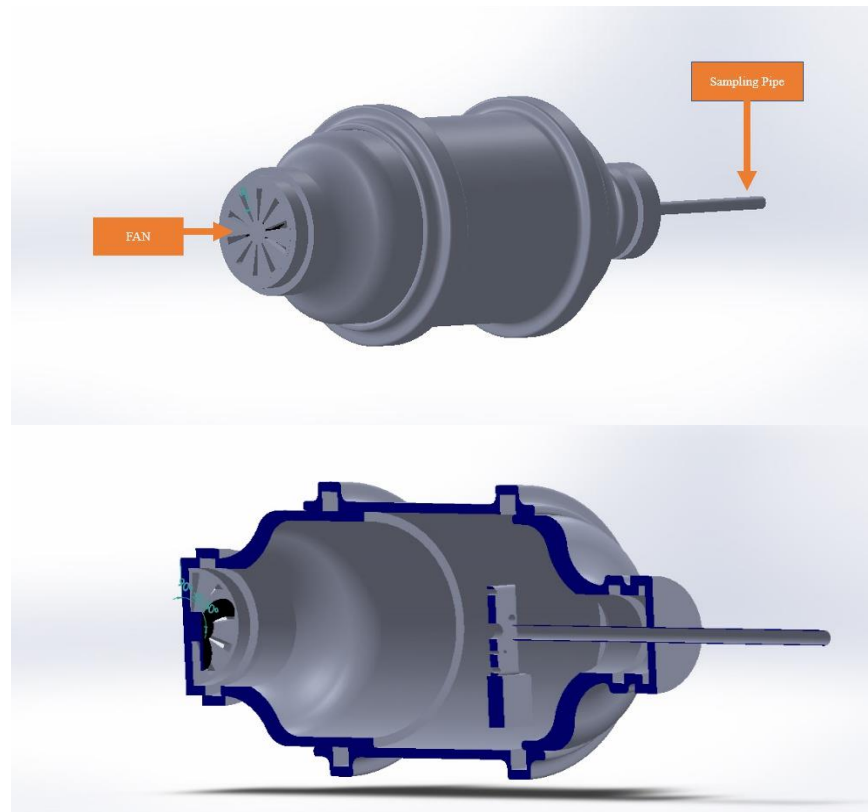


Figure 3.4-1 3D Design of Low-Cost Device

3.5 Cost of Low-cost particle filter integrity tester

| Component | Cost In Euro |
|---------------------------|--------------|
| Sharp GP2Y1010AUOF | ~10 (€) |
| Arduino Uno | ~8(€) |
| Breadboard | ~3(€) |
| Fan | ~4(€) |
| Piping System | ~8(€) |
| Wiring | ~2(€) |
| Miscellaneous | ~5(€) |
| Total Cost – 40(€) | |

Table 3.5-1 Cost Estimation of Low-Cost Device

4 Experimental setup

4.1 Validation Instruments

In an experiment, two commercially available, higher-end portable online particle concentration devices were used alongside the low-cost device to compare and validate the low-cost device. The working principle and setup are explained later in this section.

4.1.1 NanoMet3

NanoMet3 is a Portable Emissions Measurement System (PEMS) suitable for sampling, dilution, conditioning, and counting of exhaust particles from diesel and gasoline engines. NanoMet3 works on the principle of "Unipolar Charge Diffusion". It has a separate exhaust probe and a control unit to preserve the sample for accurate measurement. NanoMet3 is equipped with a Diffusion Size Classifier (DiSC) which provides the average diameter of solid particles with the size range of 10-300 nm.

Aerosol is charged in a unipolar diffusion charger by a Diffusion Size Classifier (DiSC), excess ions are removed in an ion trap. The charged aerosol passes through a diffusion stage where particles are deposited by diffusion and trapped as an electric current. The remaining particles pass to the second stage, a filter stage, where the current is also measured. The ratio of the two currents is a measure of the average particle size. The charge per particle is a function of the particle diameter, so once known, the particle number can be calculated from the total current and the flow rate. Figure 4.1-1 shows the setup of DiSC.

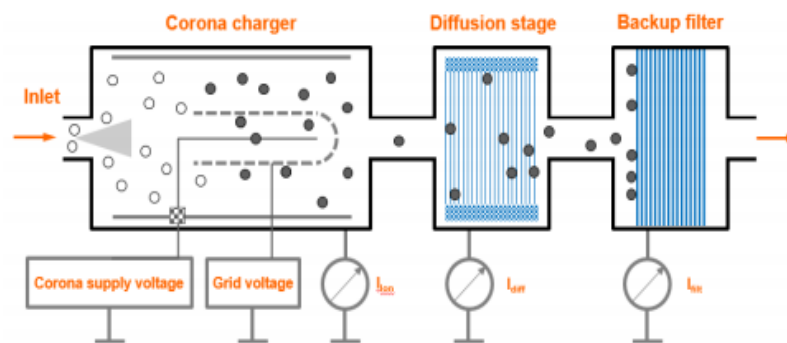


Figure 4.1-1 Unipolar Diffusion Charger [48]

NanoMet3 is combined with a diluter (Rotating Disc Diluter) and heater (~300°C) to remove volatile particles known as Post-Dilution Thermo-conditioner which is fully compliant with Particle Measurement Protocol (PMP).

4.1.2 Engine Exhaust Particle Sizer (EEPS)

The Engine Exhaust Particle Sizer is a fast response, high resolution instrument for measuring exhaust particle size distribution in the range of 5.6 to 560 nm. Due to its resolution time of 10 Hz, the dynamic behaviour of particle emissions can be investigated during transient test cycles. EEPS consists 32 size channels (16 channels per decade). [42]

Exhaust particles drawn through the inlet of the EEPS are charged to a predictable level using a corona charger. These charged particles are introduced into the high voltage electrode column and transported downward by HEPA filtered sheath air. The positively charged particles are repelled outward by a positively charged electrode due to electrical mobility and impacts on the electrometer. The particle with higher charge strikes to the top electrometer and lower one in the bottom. The electrometers used are of high sensitivity and allow continuous measurement of multiple particle sizes. Figure 4.1-2 shows working schematic of EEPS. [42]. During an experiment a thermo diluter was used to dilute the sample before EEPS.

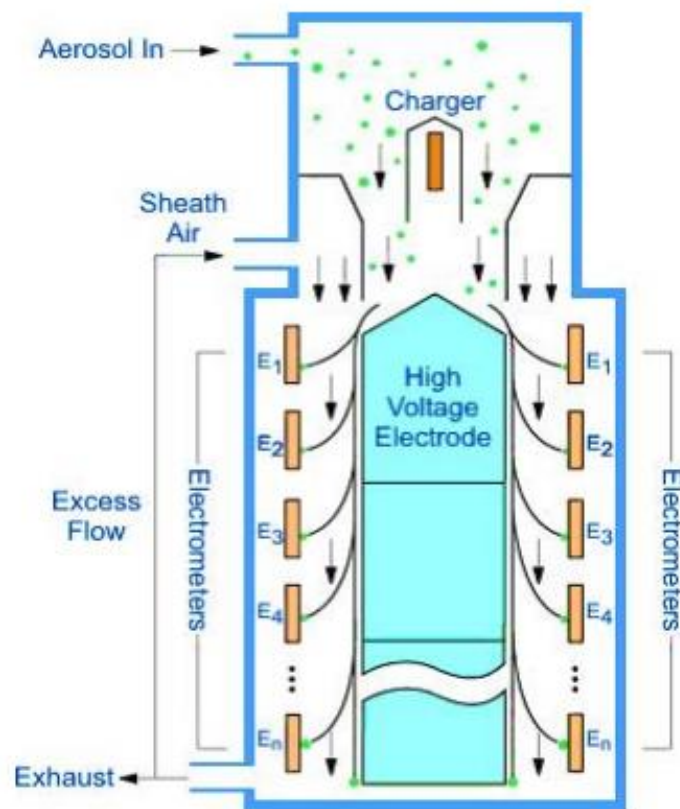


Figure 4.1-2 EEPS Working Schematic [42]

4.2 Experiment procedure

The experiments were conducted on April 21, 2021, and June 14, 2021, at Czech University of Life Sciences. The vehicle of interest in these experiments were passenger cars with and without DPF. As discussed, earlier EEPS and NanoMet 3 were used along with the low-cost device. The detailed experimental procedure is as follow:

- The experiments were conducted in four stages:
 1. Idle, no load.
 2. High idle (1500 rpm), no load.
 3. High idle (2000 rpm), no load.
 4. Free acceleration, no load.
- In each stage (except 1st stage), the exhaust probe or sampling line of all three devices were located in the exhaust pipe (tail pipe) of the vehicle. In the first stage, all three sampling lines (from all three devices) were in the exhaust pipe for a specified time and then into the atmosphere for a specified time.
- Each stage consists of four cycles, with each cycle lasting 80 seconds.
- EEPS and NanoMat 3 were in continuous operation all the time, but the low-cost device was only in operation during the measurement of individual vehicle.
- Time was noted manually using a portable stopwatch. The data were stored with respect to time.

4.3 Vehicles Used During Experiment

Prior to the start of the experiments, it was known which vehicle was with DPF and which was without DPF. Table 4.3 1 shows the vehicle model used with its condition (i.e. with DPF or without DPF).

| Vehicle Model | State |
|----------------------|--------------|
| Skoda Roomster | Without DPF |
| Skoda Octavia | Without DPF |
| Skoda Rapid | With DPF |

Table 4.3-1 Vehicle Details

4.4 Field Setup



Figure 4.3-1 Skoda Roomster Experiment Setup



Figure 4.4-2 Sampling Pipe of Three Instruments

Figure 4.4-3 shows sampling of the exhaust particles from the vehicle tailpipe to all three instruments. The volatiles can condense into nanodroplets, which are detected as particles along with non-volatile particles, so the low-cost instrument is set at an angle to prevent the sensor from condensing particles.

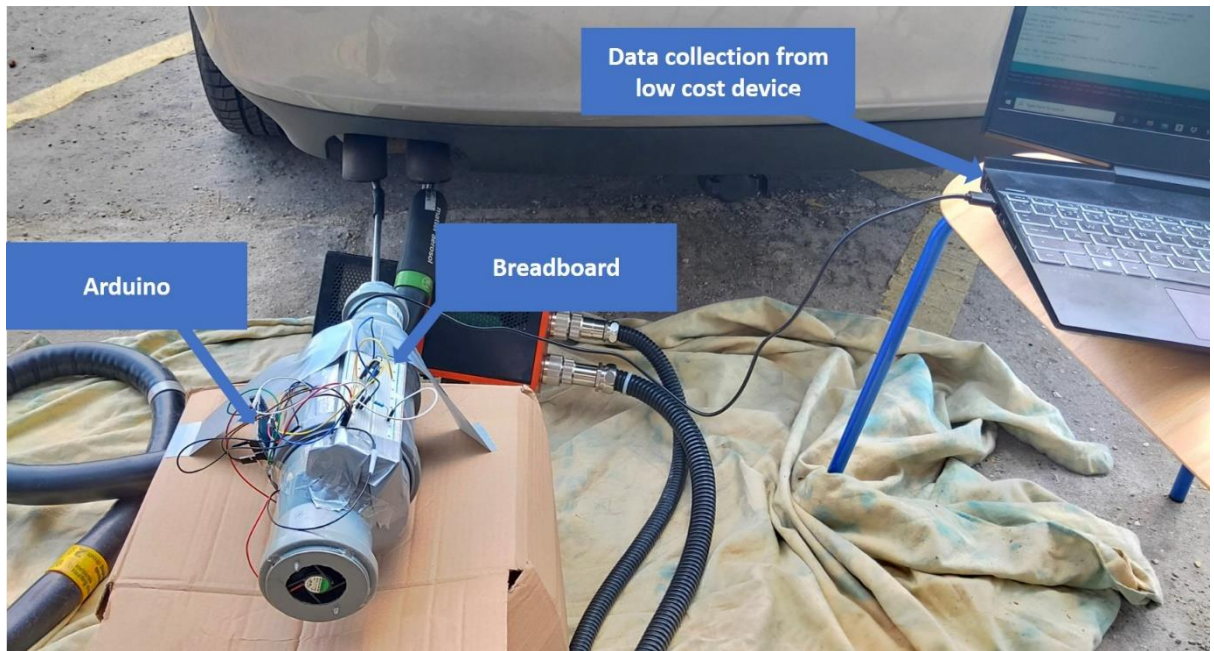


Figure 4.4-3 Sampling from Tail Pipe

4.5 Time Synchronization Between the Instruments

As discussed in an earlier section the experiment procedure consist of four stages and each stage has four cycles. So, all the instruments must be time-lined with each other during each stage and cycle. There will be some delays and advances in the output during the experiment due to the following reasons:

- The suction pressure in the sampling pipes and the sampling pipe length is different for every instrument
- During an experiment, you have to insert the sampling line from all the instruments into the tailpipe at a certain time and also take it out at a certain time, so there is a great chance for human error
- Each Instrument has its own time of response (i.e.,10Hz, 1Hz)

The NanoMet3's clock was 25 minutes ahead of the actual time during an experiment. In addition, the NanoMet3 and EEPS were in continuous operation even when no experiment was taking place. To account for this, time was manually noted during each stage and cycle. When analysing the data, the timeline was matched to the corresponding stage and cycles, additionally, a visual analysis was performed for each instrument to determine time synchronization by analysing the peak and fall valued from the respective graph. Figure 4.5-1 Shows a time synchronized graph between NanoMet3 and Sharp GP2Y1010AUOF.

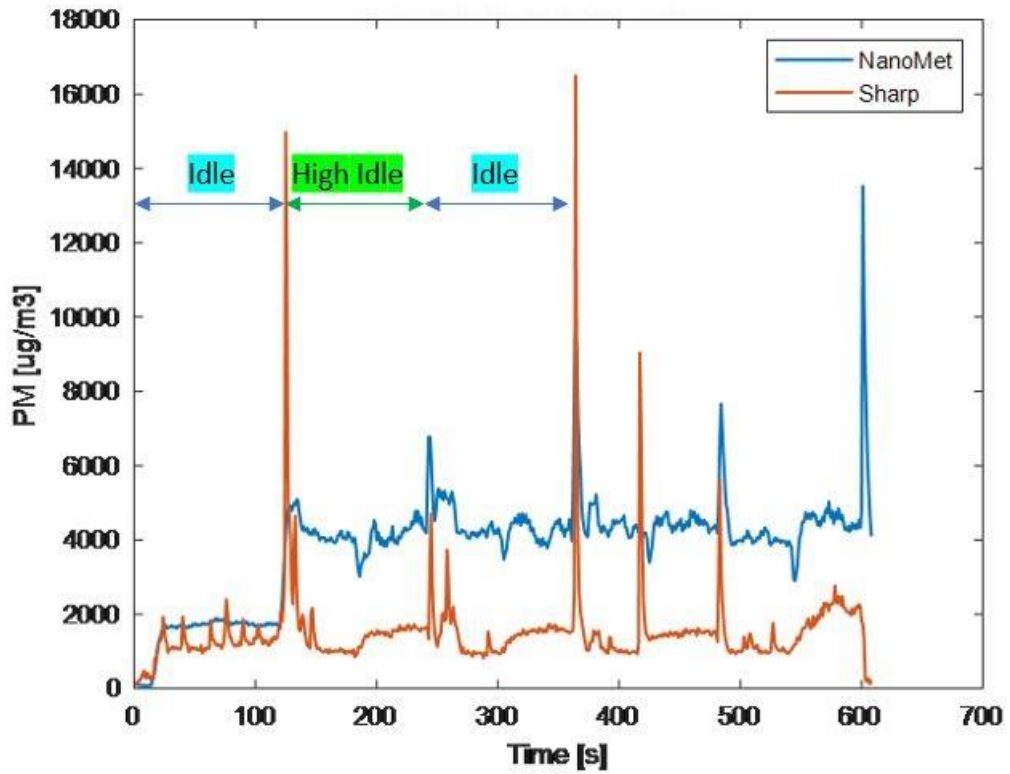


Figure 4.5-1 Time Synchronization Octavia(W/DPF)

4.6 Particle Mass from EEPS

The Engine Exhaust Particle Sizer (EEPS) gives the number of particles per cm³. The mass of the particles can be calculated by multiplying the particle density by the particle volume. Since exhaust particles are polydisperse in nature, the effective density must be considered in this case. The research indicates that the effective density of soot particles generated by diesel engines decreases as the particle size increases, ranging from 1.2 g/cm³ at 50 nm to 0.3 g/cm³ at 300 nm [43]. The particle density also depends on the engine load and engine speed [44]

In this report, the effective density was taken as 0.8 g/cm³ for the calculation purpose. The shape of the particle was assumed to be a sphere. So, the equation was given as,

$$\text{Volume of the particle , } V = 1/6 \times \pi \times D^3$$

$$m = \rho_{eff} \times V$$

Where , $D = \text{Particle Diameter}$

$\rho_{eff} = \text{Effective Density}$

4.7 Pre-processing of Data

During the experiment, the factory calibration for measuring instruments was maintained and data are expressed in $\mu\text{g}/\text{m}^3$. Data from the sharp sensor were smoothed using a MATLAB's "smoothing" command. Figure 4.7-1 Shows example of smoothen graph for one of the cycles.

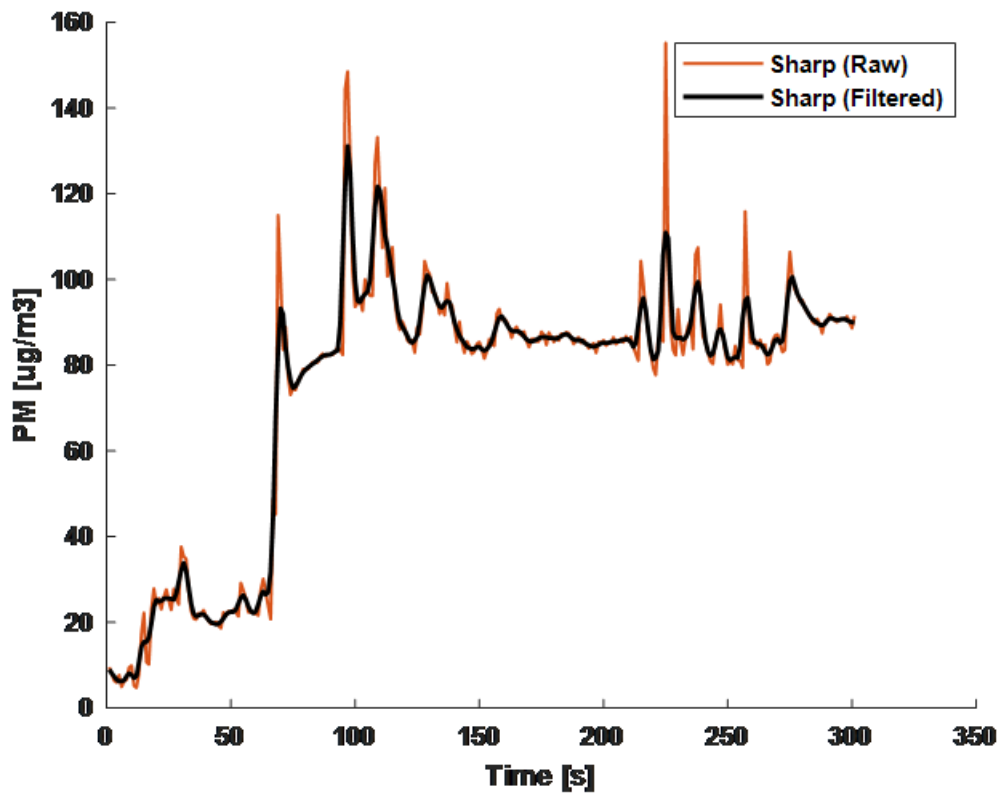


Figure 4.7-1 Data Smoothing Using MATLAB

5 Validation results

5.1 Particle Size Distribution

Particle size is the most important parameter to characterize aerosol behaviour. all properties of an aerosol depend on particle size [45] There are two types of aerosol particles, Monodisperse and Polydisperse. Monodisperse particles have uniform diameter and mass, while Polydisperse particles have different diameters and particles. Atmospheric aerosols are polydisperse with a wide range of particles.

As discussed in 4.1.2 EEPS (Engine Exhaust Particle Sizer) segregates particle number by particle diameter (Electromobility). The statistical approach was carried out on the vehicle with DPF and without DPF and the graphical representation of particle size distribution was created.

5.1.1 Particle Size Distribution for Vehicle with & without DPF

Figure 5.1-1, Figure 5.1-2, Figure 5.1-3, Figure 5.1-4 Shows the particle diameter (in nm) and the corresponding number of particles for each stage. The data were analyzed from Engine Exhaust Particle Sizer. From the figure, it can be seen that the number of particles is highest at a particle diameter of 10-20 nm, possibly due to the fact that the vehicle is at no-load condition and nucleation taking place. The second peak takes place at a particle diameter of 60-80 nm which indicates that the vehicle is without DPF. For vehicle with DPF there is no second peak which shows clearly that vehicle is equipped with DPF.

Particle distribution was created by taking the average of particle counts accumulated in each channel (or bin) during four full cycles, i.e., ~320 seconds/stage. One cycle consists of ~80 seconds. During high idle, let us assume at 2000 rpm, the engine runs at 2000 rpm for every 40 seconds out of 80 seconds, but during free acceleration, free acceleration occurs for only 3-5 seconds in a cycle. But as stated earlier, the average was taken over the entire 320 seconds, so if the period of averaging for free acceleration is shortened by considering only the period of response to free acceleration, then the concentration will be higher during free acceleration. For consistency of calculations, all stages are calculated in the same way here.

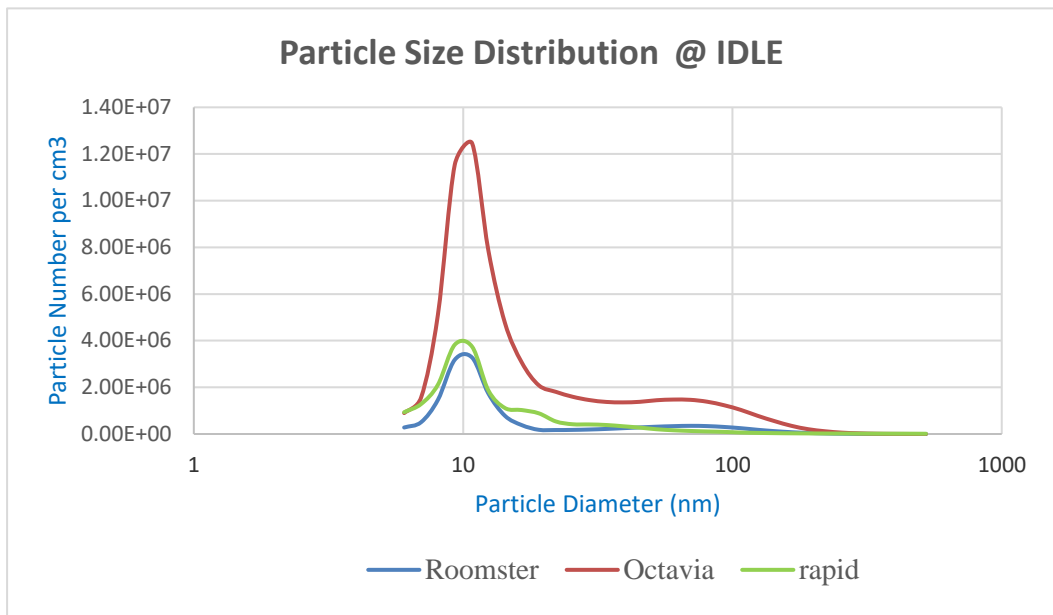


Figure 5.1-1 Particle Size Distribution IDLE

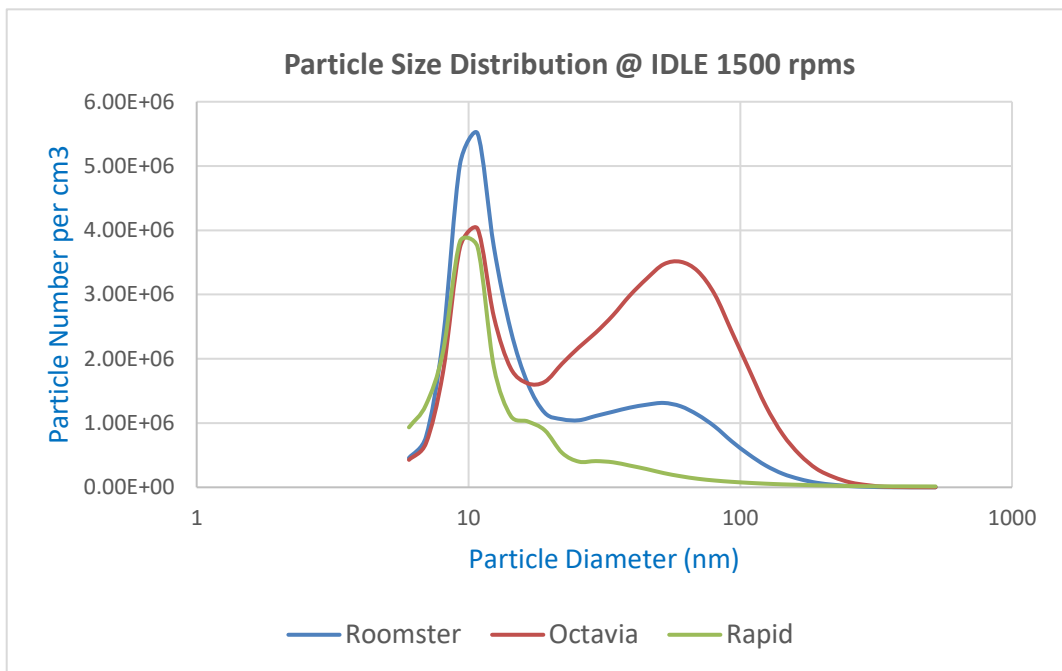


Figure 5.1-2 Particle Size Distribution IDLE 1500 rpm

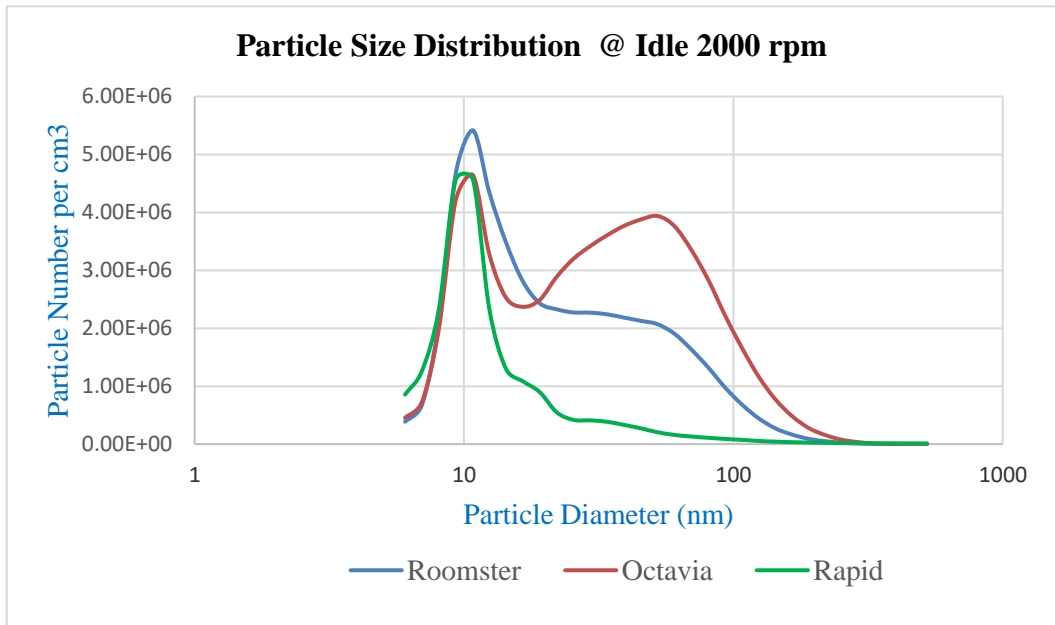


Figure 5.1-3 Particle Size Distribution IDLE 2000 rpm

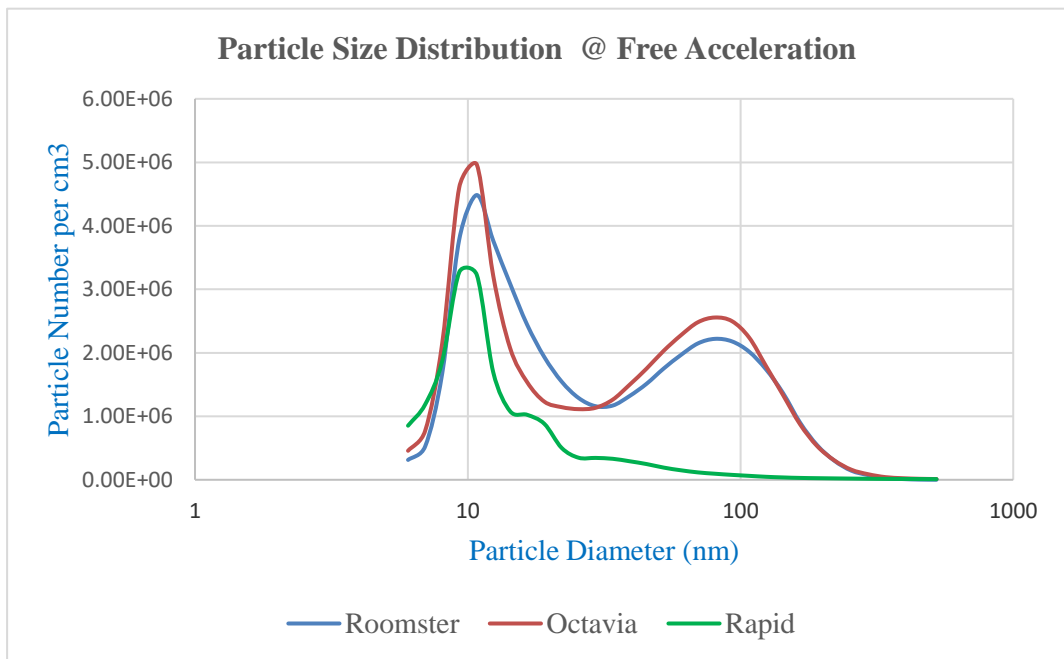


Figure 5.1-4 Particle Size Distribution Free Acceleration

5.2 Gain Factor

The data from the low-cost device were multiplied by a gain factor to achieve maximum agreement with the EEPS and NanoMet3 data. The gain factor is purely based on the observation of the graph pattern. The gain factor is chosen where the graph pattern of the low-cost device maximally matches EEPS or NanoMet3. Each vehicle may have a different gain factor. Here, a gain factor of 10 is used for Roomster & 50 for Octavia is used.

Figure 5.2-1 shows a comparison between NanoMet3 and Low-cost device for Octavia at high idle without a gain factor whereas Figure 5.2-2 is with the gain factor of 50.

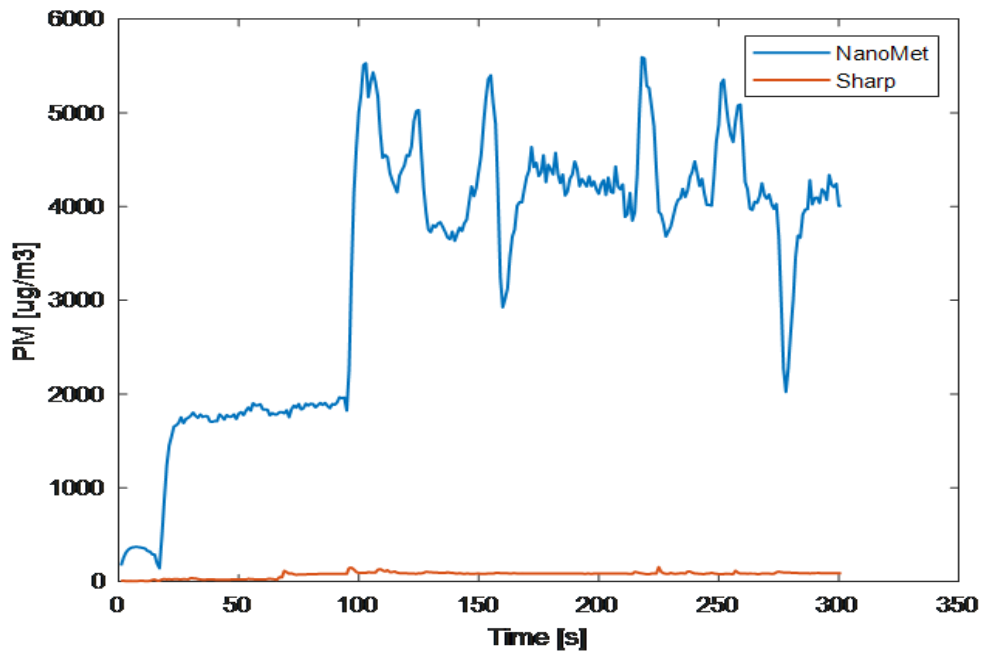


Figure 5.2-1 High Idle Stage without Gain Factor (Octavia)

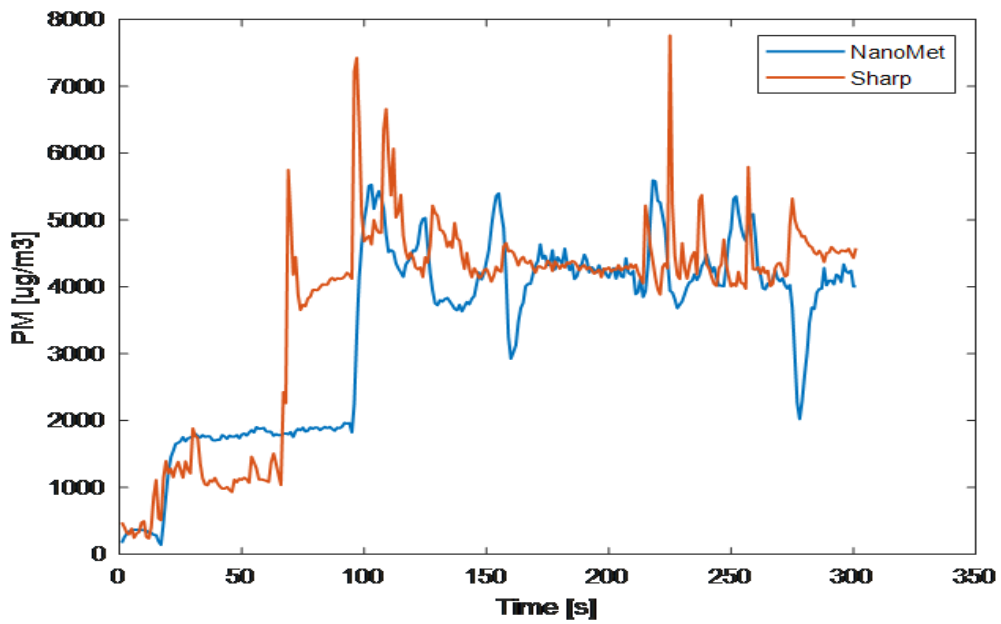


Figure 5.2-2 High Idle Stage with Gain Factor (Octavia)

5.3 Comparison Among Instruments

As described in section 4.1, NanoMet3 and EEPS were used together with the low-cost device as a reference device. This section focuses on the comparison among these three devices. Comparison during the idle phase for all three vehicles i.e., Octavia, Roomster, and Rapid, the probes of all three devices were held in the atmosphere for approximately 40 seconds and then inserted into the tailpipe of the vehicle for another 40 seconds. This procedure was repeated four times (i.e., four cycles).

Here in Figure 5.3-1 & Figure 5.3-3 the letter A stands for the fact that the probe was in the atmosphere for this period and the letter B stands for the fact that the probe was in the tailpipe of the vehicle.

In the case of the Octavia vehicle, the cold start was performed before the idling phase. From Figure 5.3-2, it can be seen that there is a sharp increase initially, indicating a cold start. The vehicle was warmed up and then the idle cycle was performed.

Again, note that Roomster and Octavia were equipped with a non-functioning DPF and Rapid was equipped with a functioning DPF.

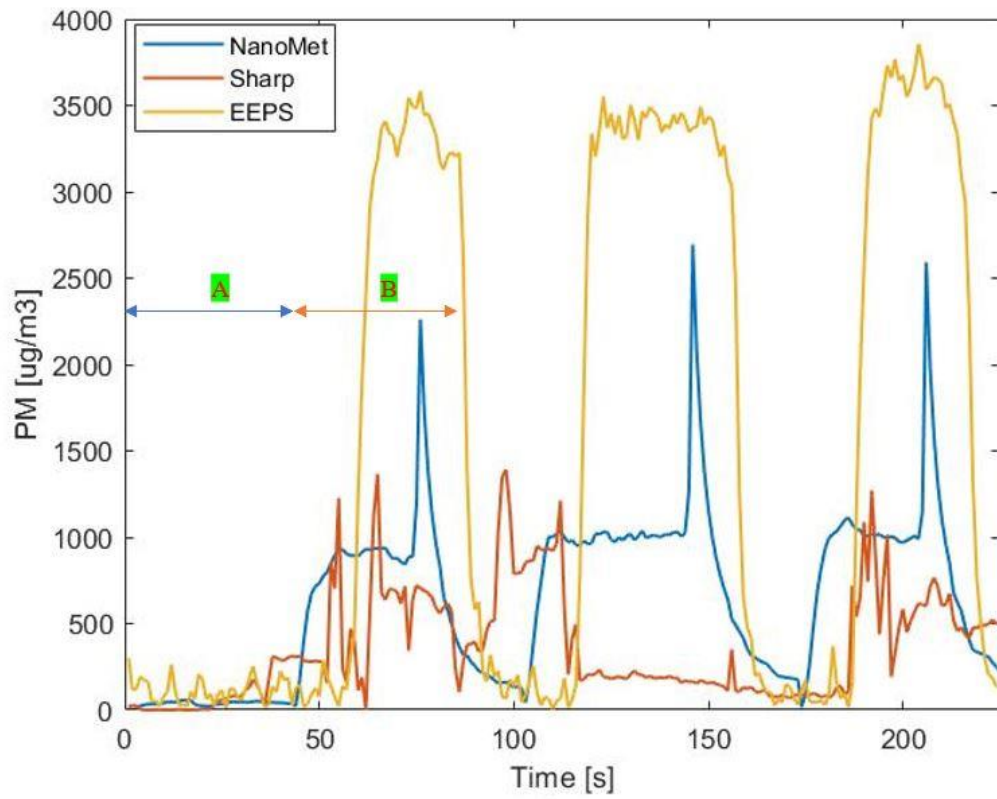


Figure 5.3-1 Comparison Among Three Instruments Roomster Idle (No Load)

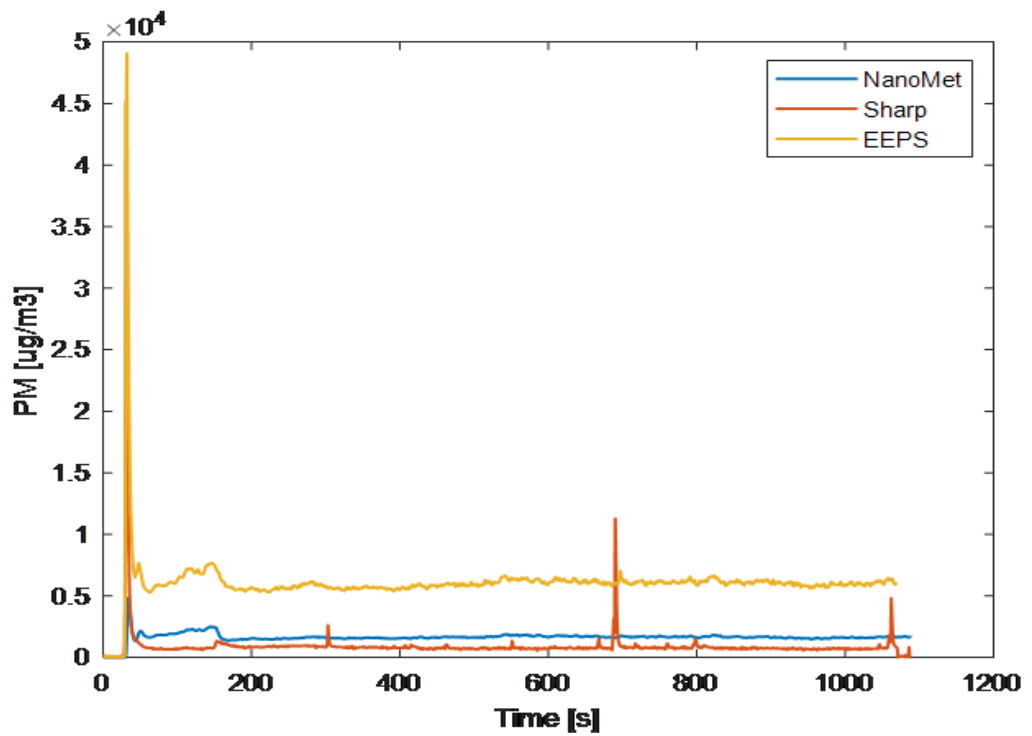


Figure 5.3-2 Comparison Among Three Instruments – Octavia Cold+idle

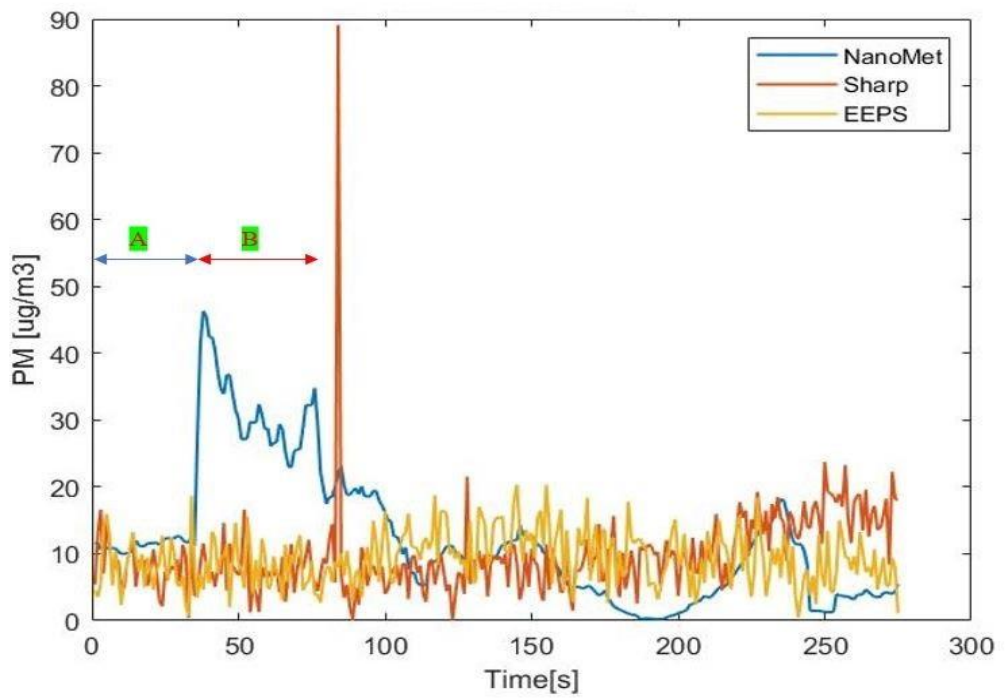


Figure 5.3-3 Comparison Among Three Instruments - Rapid (Idle)

During high idle the probe from all three instruments remains inside the tail-pipe of the vehicle throughout the whole cycle. Figure 5.3-4, Figure 5.3-5 & Figure 5.3-6 shows High Idle (1500rpm) cycles for all three vehicles.

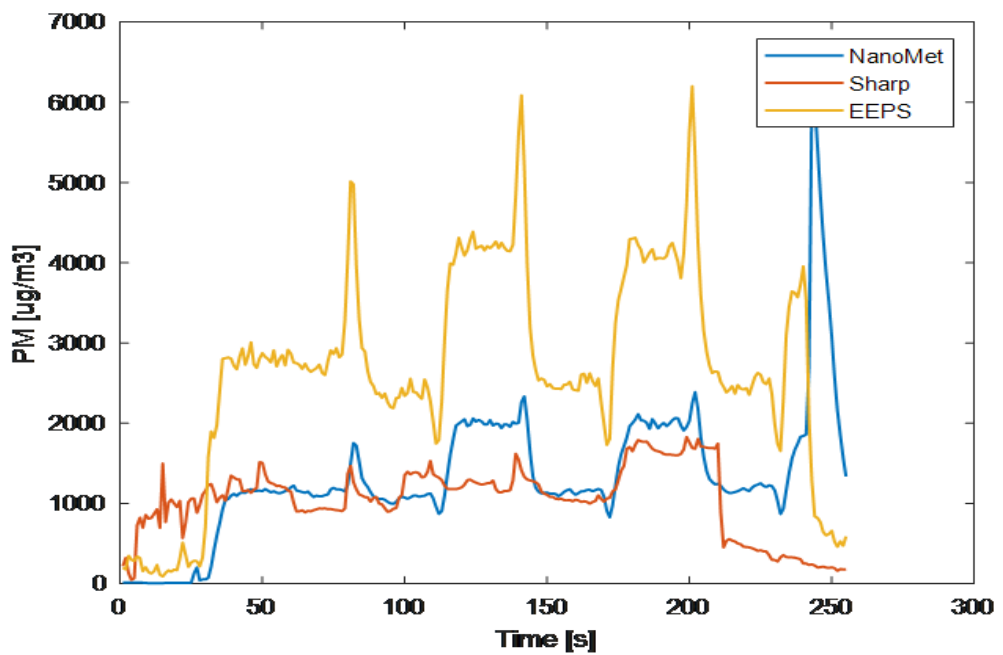


Figure 5.3-4 High Idle (1500), No load- Roomster

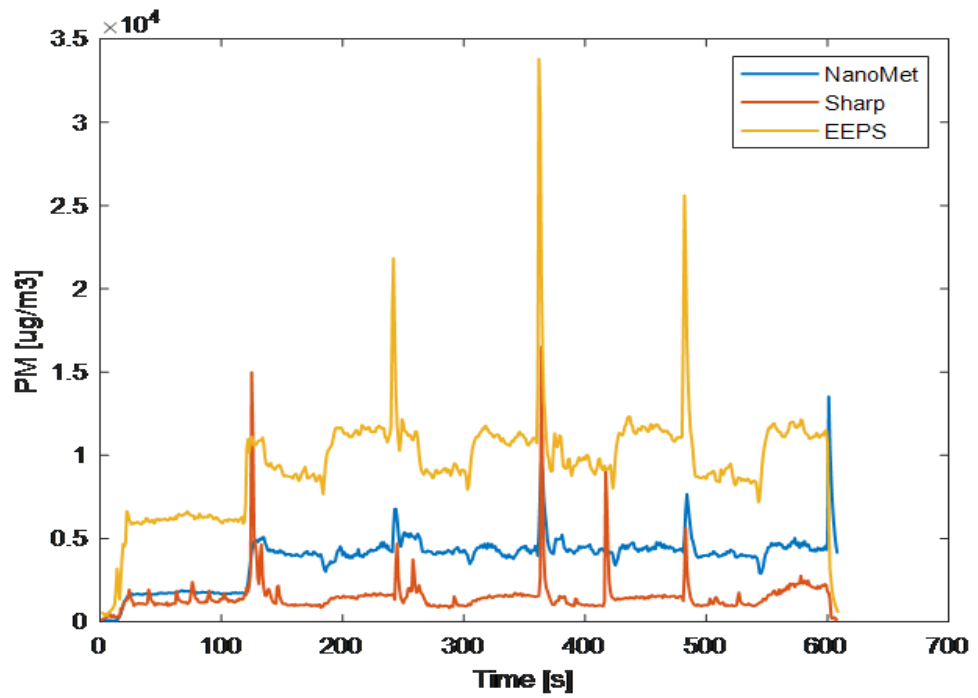


Figure 5.3-5 High Idle (1500), No load - Octavia

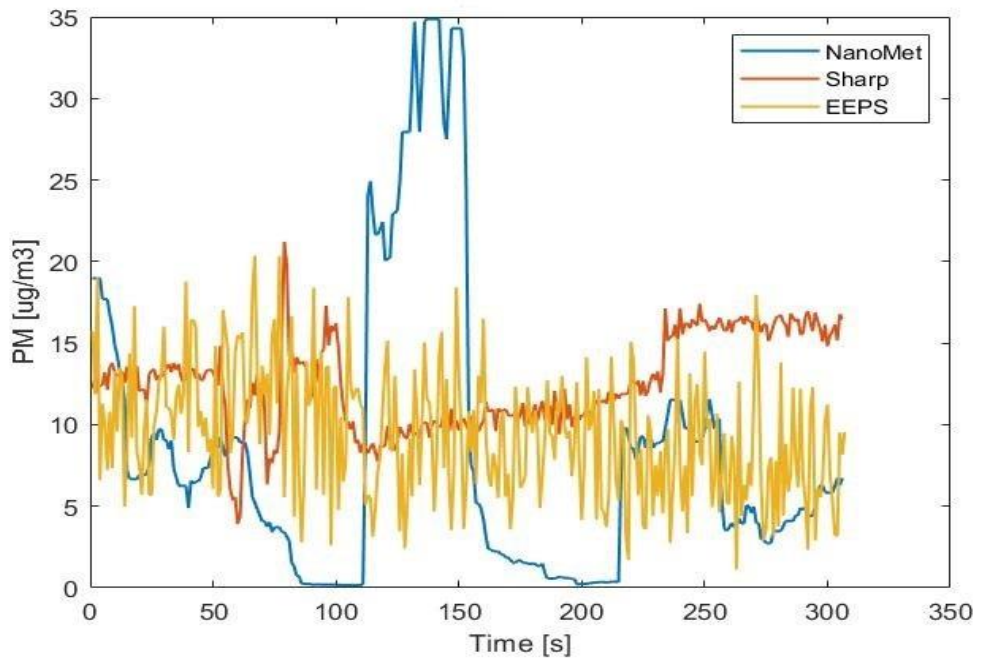


Figure 5.3-6 High Idle (1500), No Load - Rapid

Figure 5.3-7, Figure 5.3-8 & Figure 5.3-9 shows High Idle (2000 rpm) and no-load cycles for all three vehicles

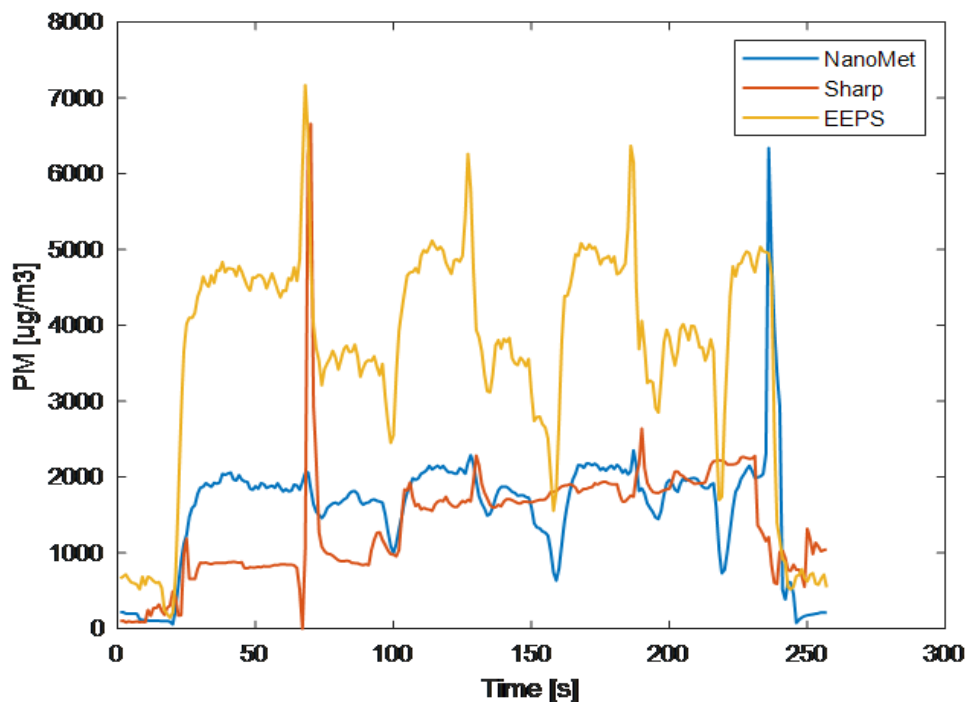


Figure 5.3-7 High Idle (2000), No Load - Roomster

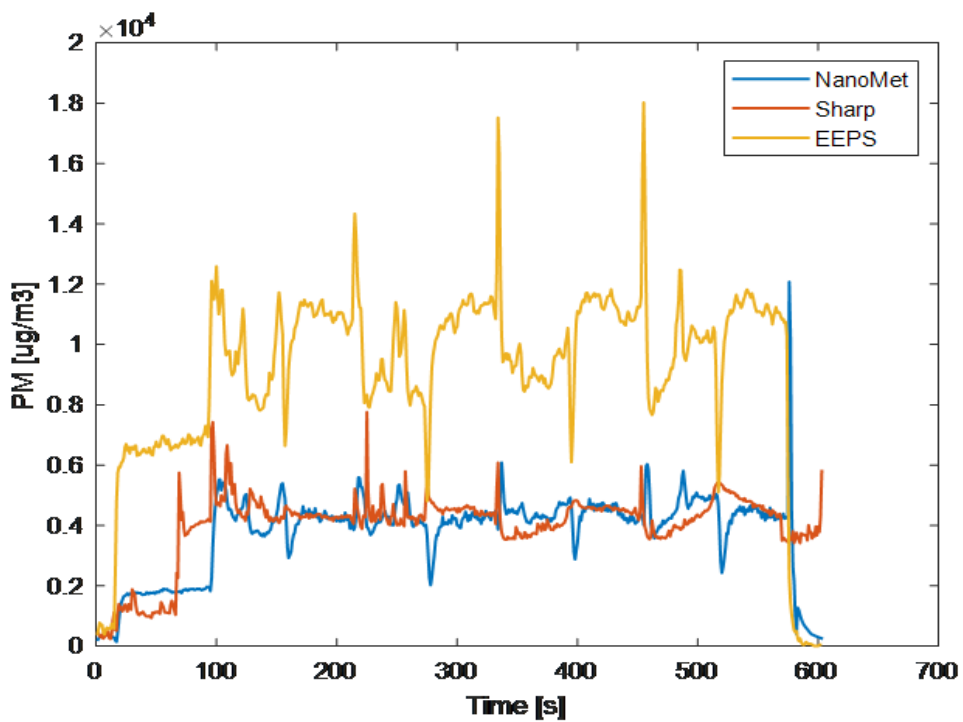


Figure 5.3-8 High Idle (2000), No Load - Octavia

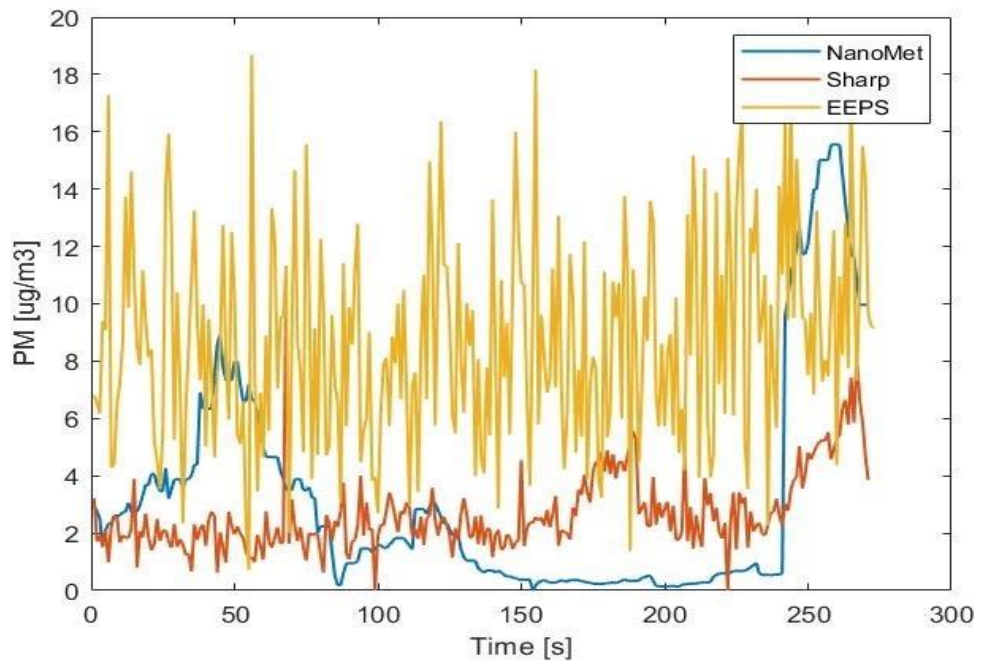


Figure 5.3-9 High Idle (2000), No Load - Rapid

Figure 5.3-10, Figure 5.3-11, Figure 5.3-12 shows free acceleration, no-load cycles for all three vehicles. It can be seen that Instruments has maximum correlation at free acceleration followed by High Idle.

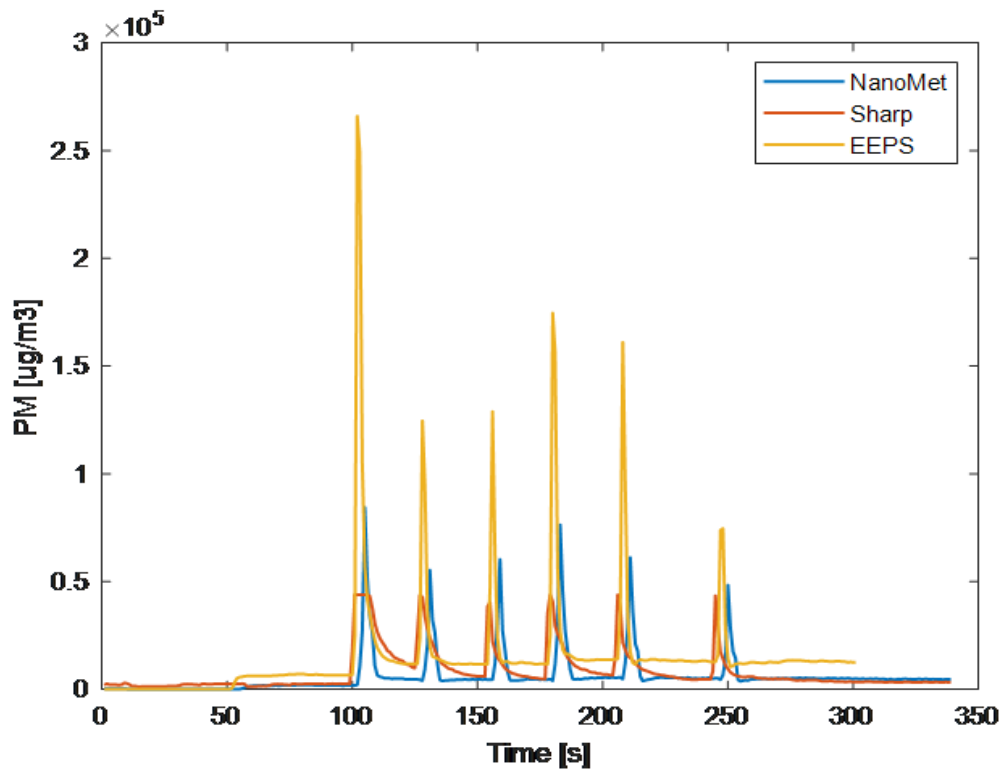


Figure 5.3-10 Free Acceleration, No Load - Octavia

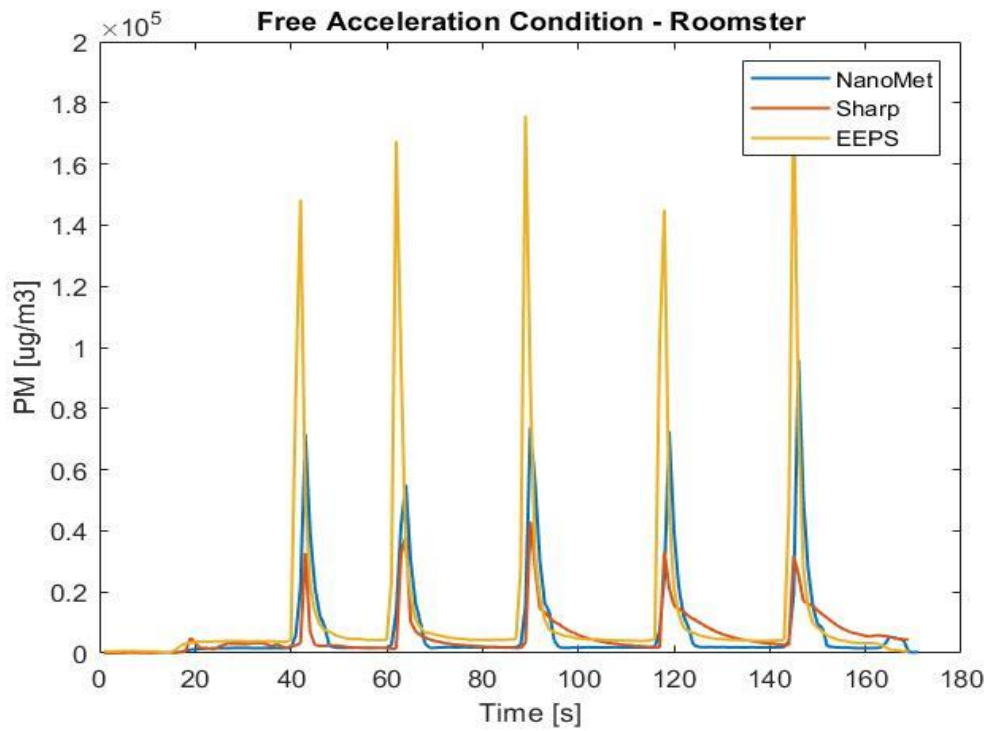


Figure 5.3-11 Free Acceleration, No Load - Roomster

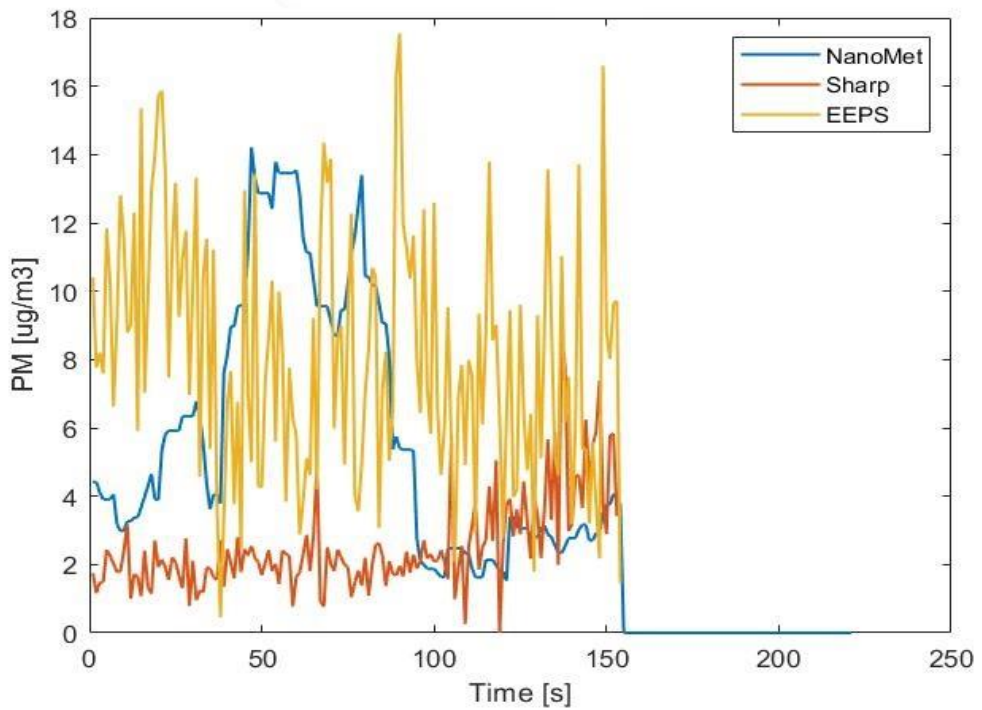


Figure 5.3-12 Free Acceleration, No Load - Rapid

5.4 Repeatability

Repeatability of measurements refers to the variation in repeated measurements made on the same individual under identical conditions. During an experiment, four identical cycles were performed on a single vehicle. Repeatability between three instruments was calculated by taking an average of the PM for each cycle and then calculating the standard deviation for the average of each cycle. The calculation was done for both the car with DPF and the car without DPF. The following equation shows the mathematical procedure for the same:

$$PM_{AVG} = \frac{\sum_{i=1}^n PM_n}{n}$$

Where n = number of readings per cycle (~320), Here PM_{AVG} shows the average of one cycle. Then total particulate matter average (TPM_{AVG}) was calculated by taking an average of four cycles.

$$TPM_{AVG} = \frac{\sum_{i=1}^4 PM_{AVG_i}}{4}$$

A standard deviation was calculated for the average of four cycles, which is shown below.

$$\sigma = \frac{\sqrt{PM_{AVG} - TPM_{AVG}}}{\sqrt{N}}$$

Figure 5.4-1 & Shows the repeatability of three instruments for a vehicle without DPF.

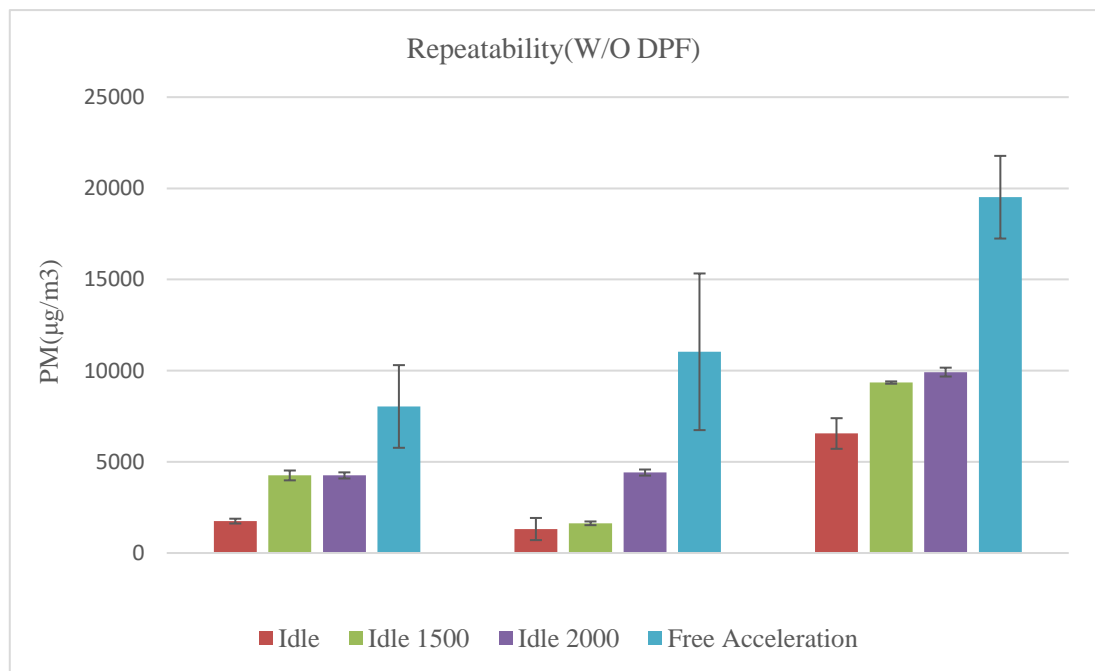


Figure 5.4-1 Repeatability of Three Instruments at Different stages (W/O DPF)

From Figure 5.4-1 it can be seen that the three sensors show higher deviation at free acceleration. The reason is the same which was discussed in section 5.1.1 that the free acceleration occurs for only 3-5 seconds in a cycle. But the average was taken over the entire 320 seconds. so, if the period of averaging for free acceleration is shortened by considering only the period of response to free acceleration then the deviation at free acceleration will be lower which can be seen in Figure 5.4-2 where free acceleration a period of averaging is shortened(~10s).

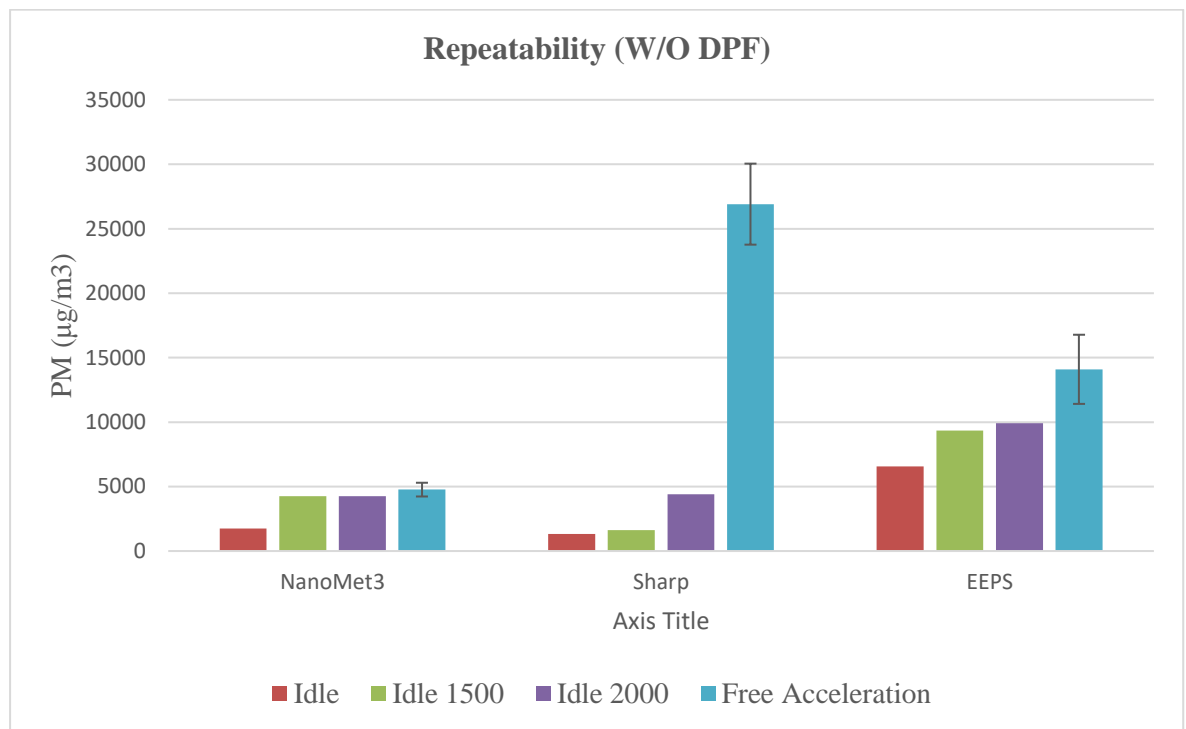


Figure 5.4-2 Repeatability of Three Instruments at shorter Interval of Free Acceleration (W/O DPF)

The reason behind the different values among instruments is that each Instrument measures a different property of the PM.

Figure 5.4-3 shows the repeatability of three Instruments for a vehicle with DPF. In the case of the DPF, the averaging interval for free acceleration is not shortened because the concentrations were already low and there was not much difference between a shortened interval and a normal interval.

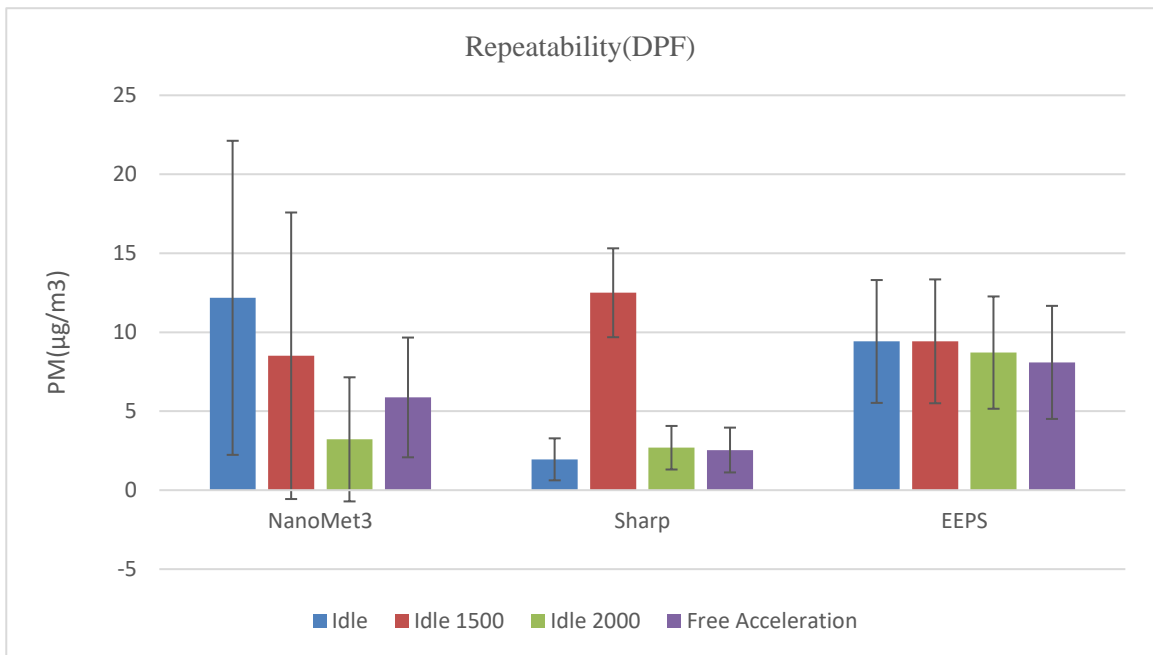


Figure 5.4-3 Repeatability of Three Instruments at Different stages (DPF)

5.5 Detection Limit

The limit of detection (LOD) is defined as the lowest limit that deviates significantly from the signal obtained from blank measurements [34]. The detection limit for the instrument will not be the same in an open environment which is provided by a manufacturer, so it is critical to determine the limit of detection to discriminate between a signal and a blank sample.

The detection limit of the sharp sensor is determined by using Kaiser and Specker approach:

$$LOD = \frac{3 \times \sigma}{K}$$

Where σ = Standard deviation at blank sample

And K is a sensitivity slope of the linear response of the sensor to different PM mass concentrations. The standard deviation is measured by placing the sensor in an isolated chamber filled with air purified by HEPA filters. The value of K can be obtained from the report of Wang et al. [34] in which incense was used as a particle source and the value of K was determined at different mass concentration ranges (0-1000 $\mu\text{g}/\text{m}^3$ and 0-100 $\mu\text{g}/\text{m}^3$), the LOD was found approximate 26 $\mu\text{g}/\text{m}^3$.

6 Discussion

6.1 Differentiating between Vehicles with DPF & without DPF

This work aimed to investigate whether the low-cost device can distinguish between a working and a non-working particle filter. The following summary graph shows how the low-cost device behaves when the particle filter is present and absent during all stages (No Load conditions).

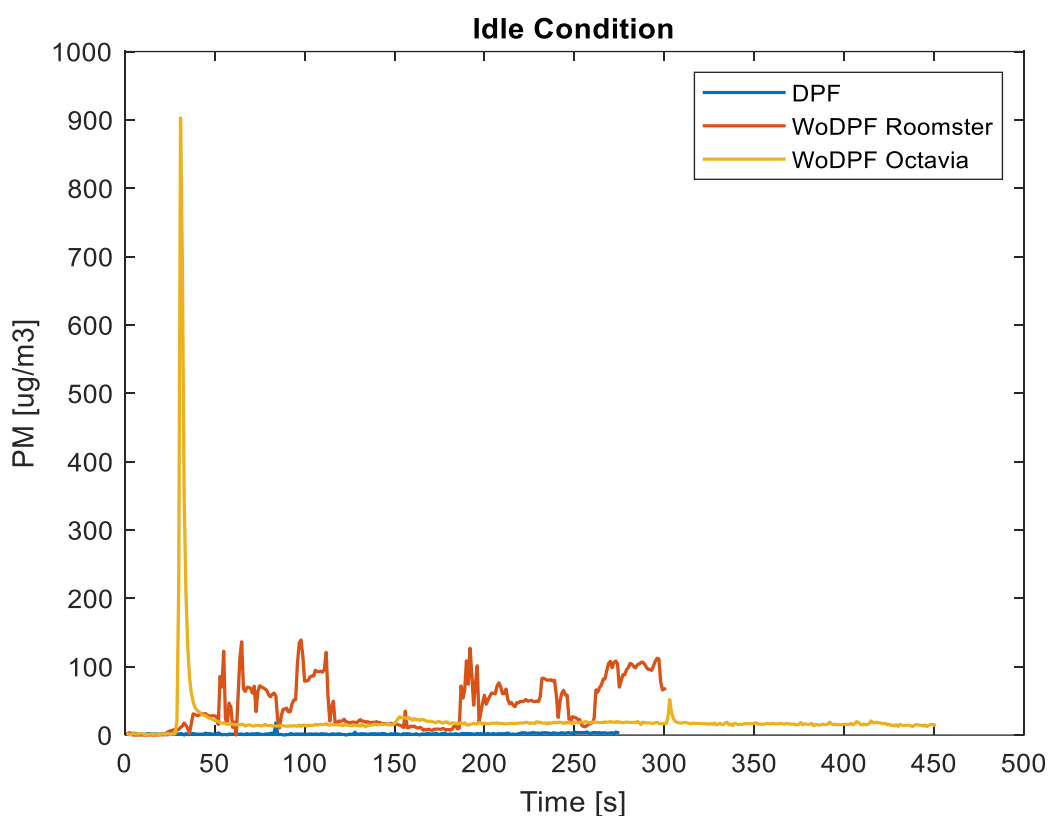


Figure 6.1-1 Low-cost device at Idle

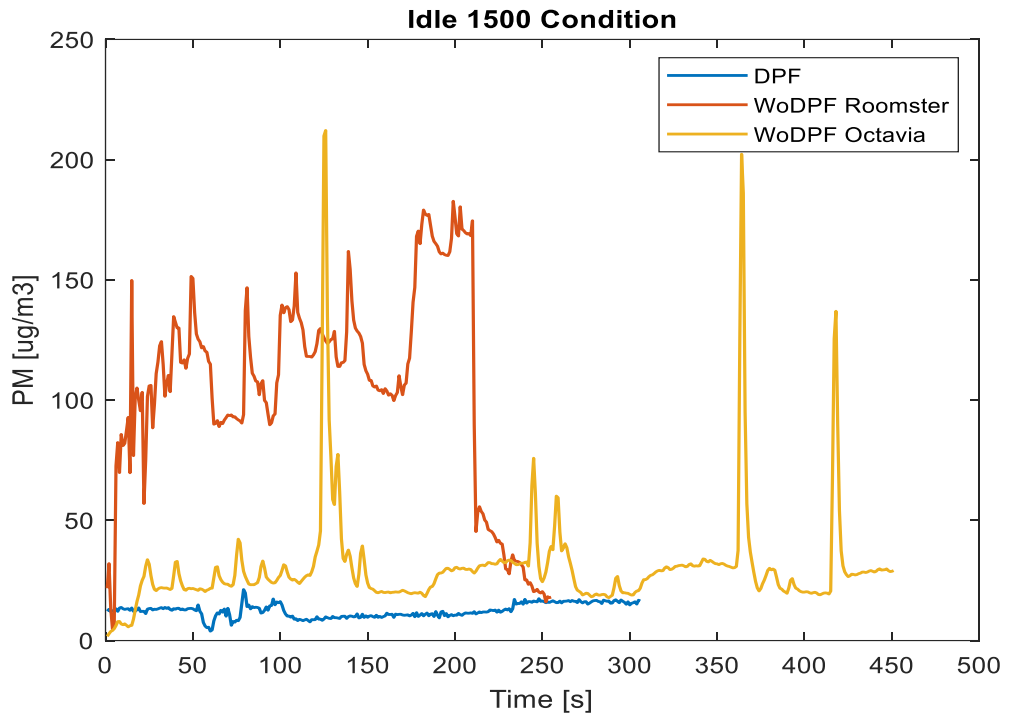


Figure 6.1-2 Low-cost Device at Idle 1500 RPM

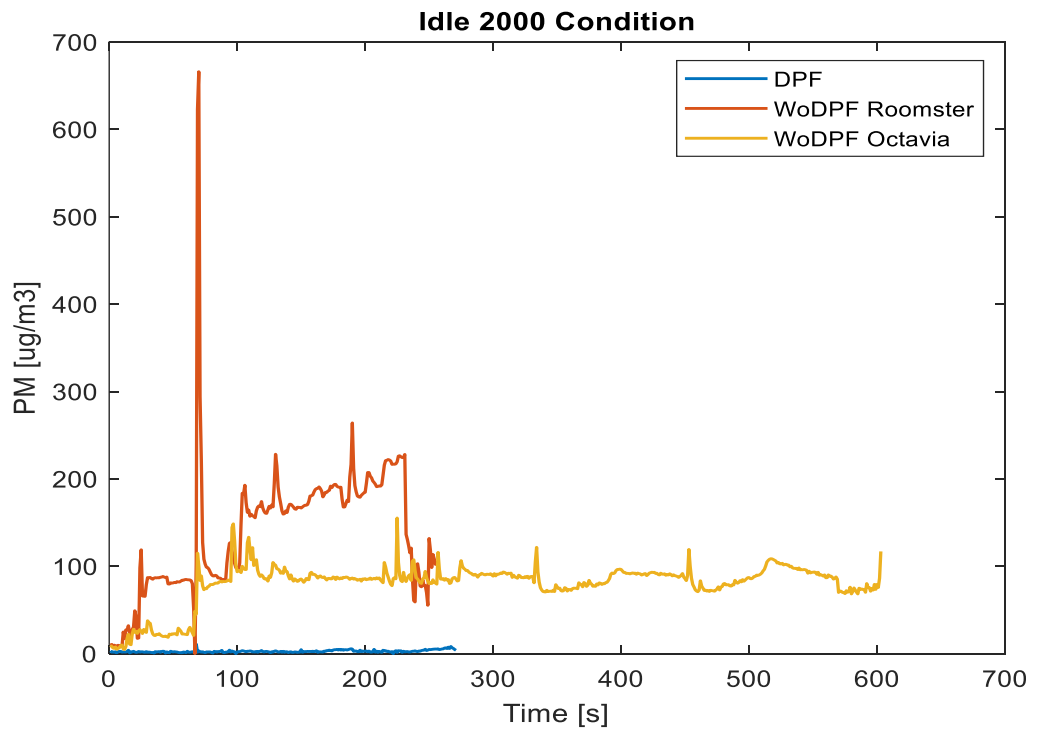


Figure 6.1-3 Low-cost Device at Idle 2000 RPM

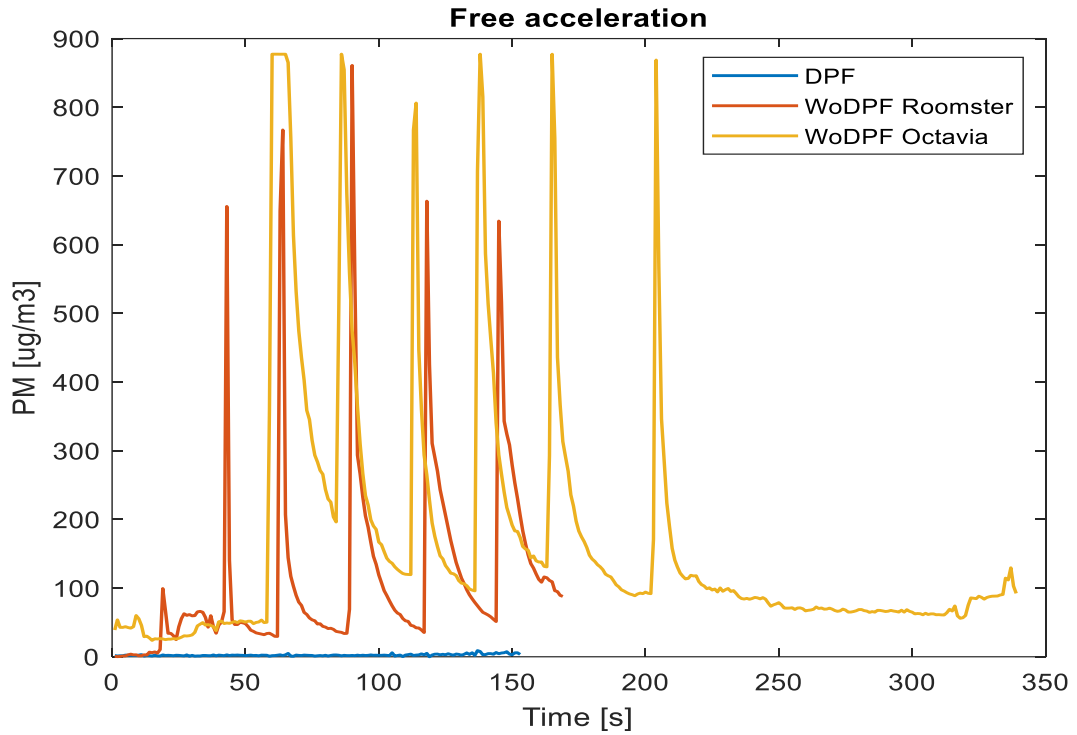


Figure 6.1-4 Low-cost Device at Free Acceleration

It is clear From Figure 6.1-1, Figure 6.1-2, Figure 6.1-3 & Figure 6.1-4 that there is a large difference in the concentration displayed by the low-cost device for vehicles with DPF and vehicles without DPF, from which it can be concluded that the low-cost device can distinguish between a perfectly functioning DPF and a non-functional DPF at each stage.

In addition to a graphical approach, a statistical approach was also used to determine the difference between a functioning DPF and a non-functional DPF. For this purpose, a student's T-test [46] was conducted. The equation used to determine the value of T is shown below,

$$T = \frac{|\bar{x}_1 - \bar{x}_2|}{\sqrt{\frac{\sigma^2_1}{N_1} + \frac{\sigma^2_2}{N_2}}}$$

Two samples were taken, one set of data from the vehicle with working DPF and another set of data from the vehicle with non-functional DPF for each stage.

Where \bar{x}_1 is the average of data taken from samples 1 and \bar{x}_2 is the average of data taken from sample 2, σ^2_1 and σ^2_2 is a variance of sample 1 and sample 2. N_1 and N_2 is the amount of data from sample 1 and sample 2 respectively.

With the T-test we have two hypotheses (two-tailed test):

1. Null Hypothesis - Null Hypothesis says there is no significant difference between two samples ($p > 0.05$)
2. Alternative Hypothesis – Alternative Hypothesis says there is a significant difference between two samples ($p < 0.05$)

The T-test was performed for each stage (e.g., idle, idle 1500...) and the probabilities found were all many orders of magnitude (average $\sim 10^{-27}$), which is < 0.05 and falls under the alternative hypothesis for each stage, which suggests that there is a large significant difference between two samples at each stage. So, with both graphical and statistical approach was used to prove that there is a significant difference between data of vehicle with DPF and without DPF from the low-cost device.

Figure 6.1-5 shows the bar chart of the average data from the low-cost device for vehicles with functional DPF and non-functional DPF for each stage, showing a clear difference between vehicles with DPF and vehicles without DPF.

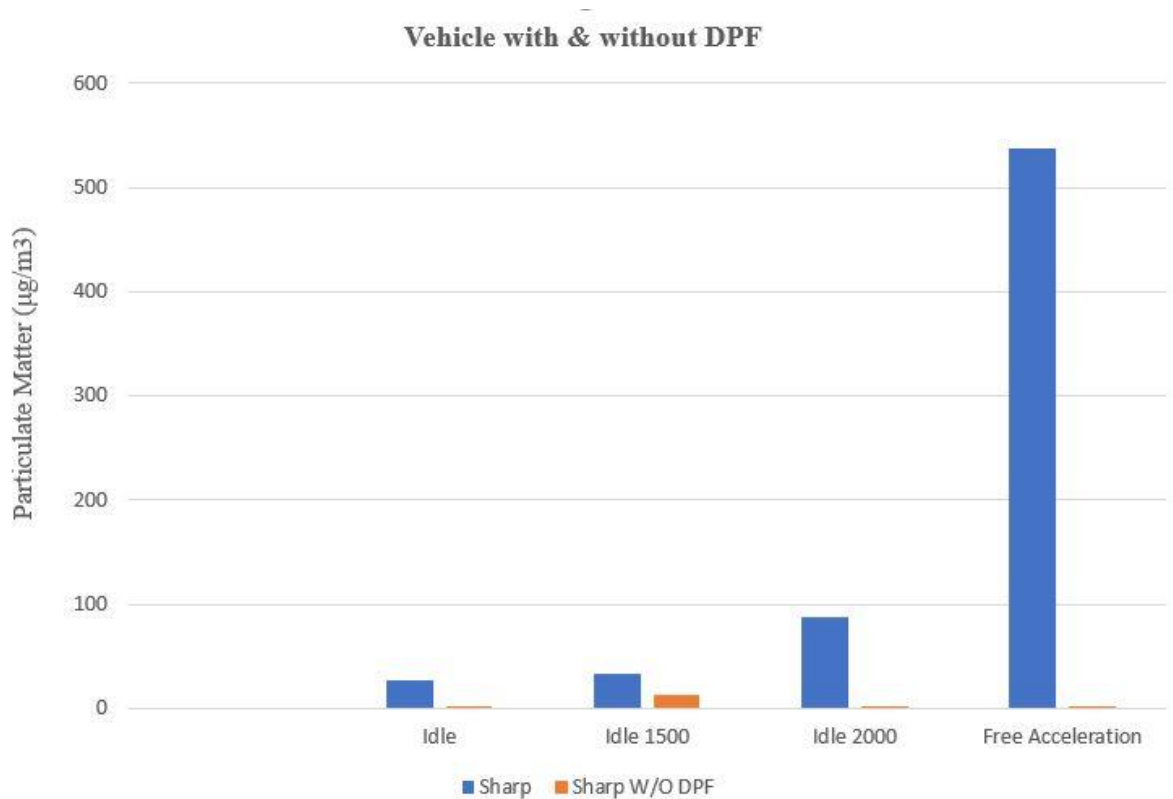


Figure 6.1-5 Average Values for Vehicle with & without DPF

Figure 6.1-6, Figure 6.1-7, Figure 6.1-8, Figure 6.1-9 shows scattered graphs of low-cost devices vs NanoMet3 on a logarithmic scale. The blue dots show the data from the vehicle equipped with DPF and the orange dots show the data for the vehicle with DPF.

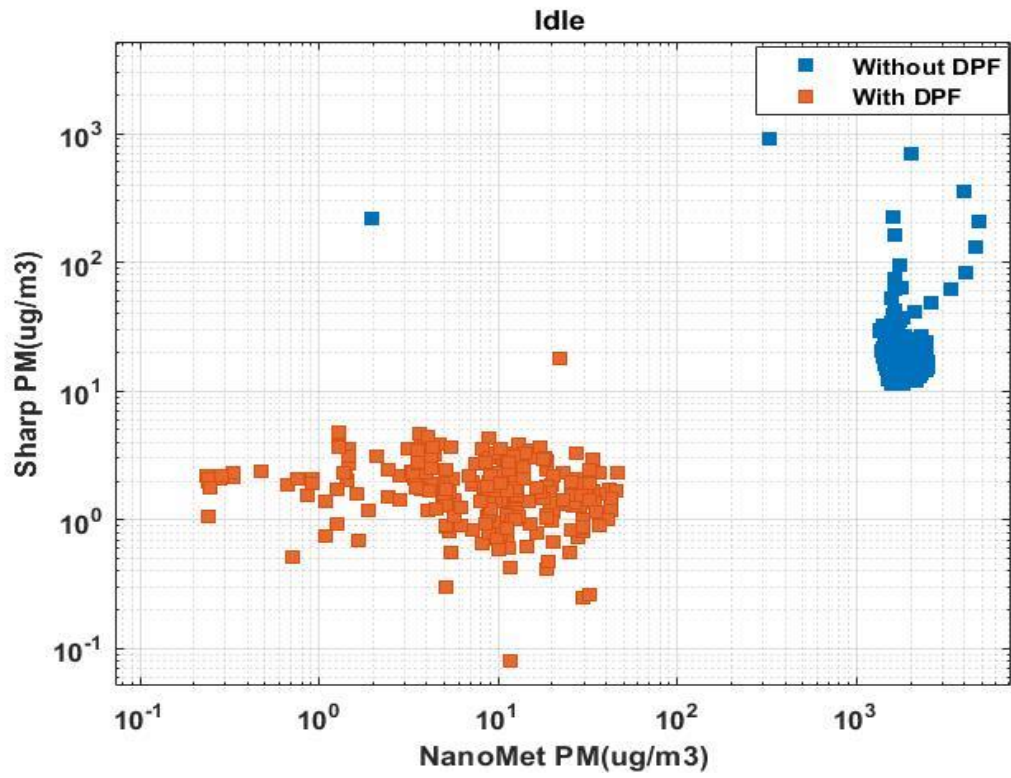


Figure 6.1-6 Scatter Graph on a Logarithmic Scale - Idle

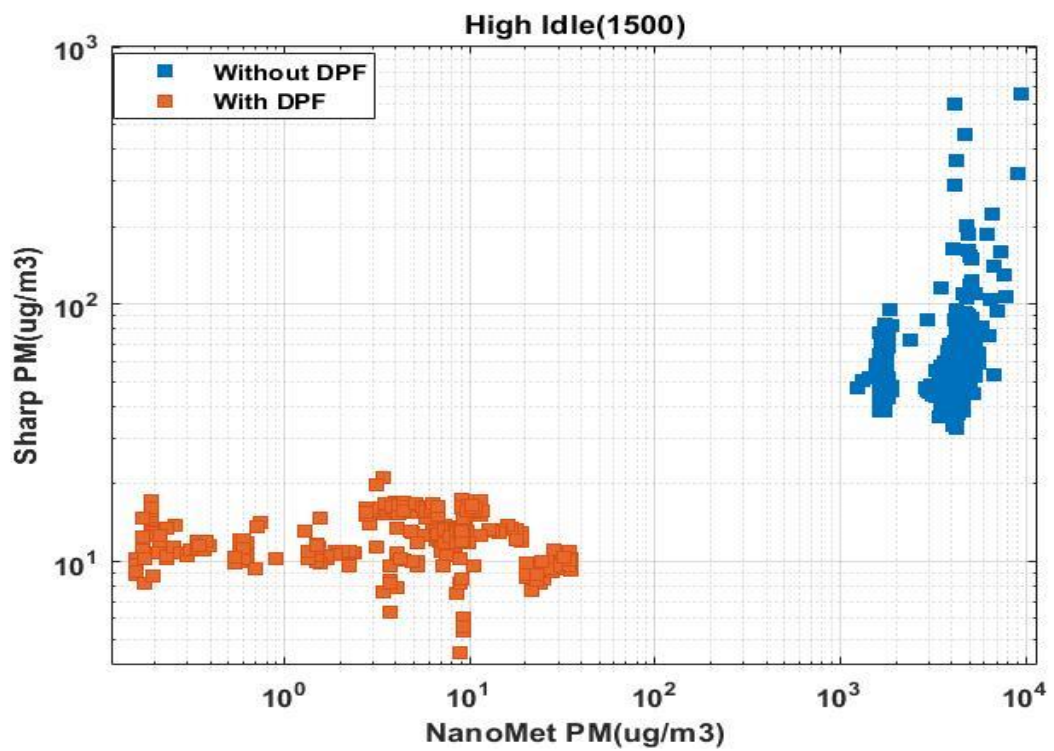


Figure 6.1-7 Scatter Graph on a Logarithmic Scale -High Idle(1500 rpm)

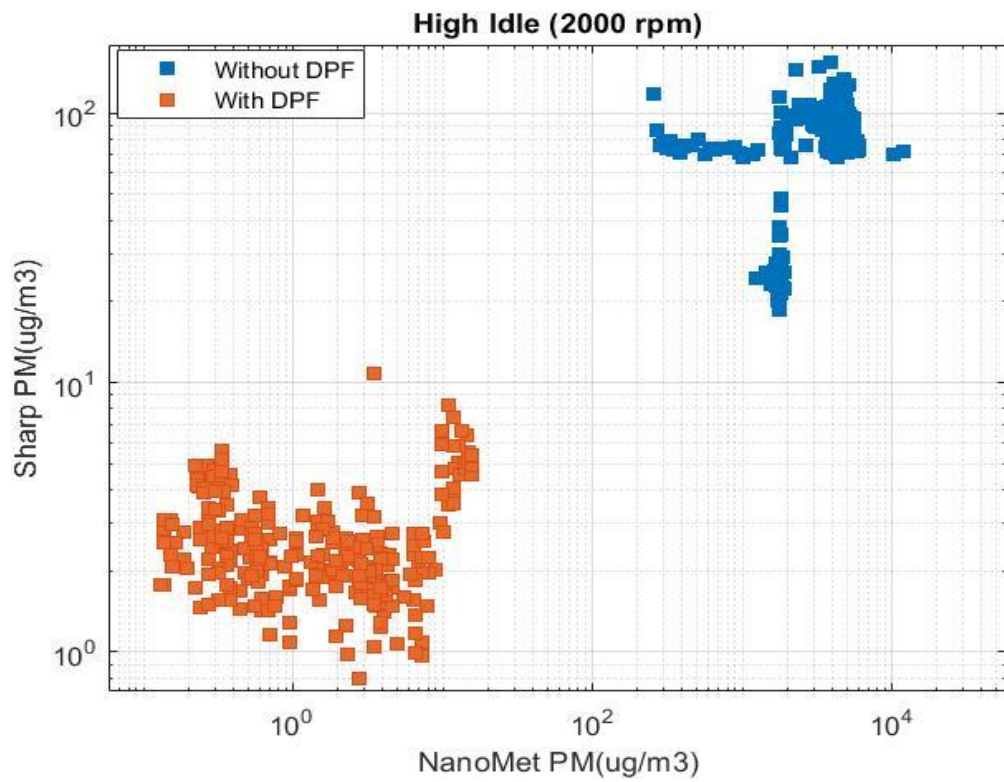


Figure 6.1-8 Scatter Graph on a Logarithmic Scale -High Idle (2000 rpm)

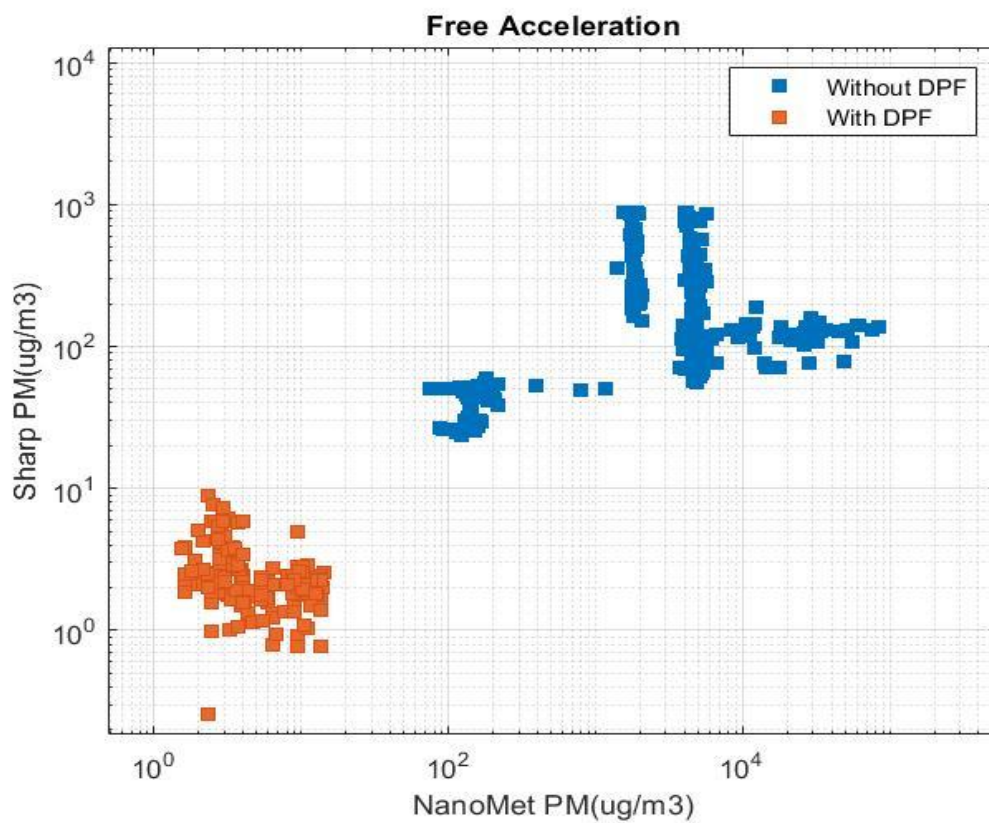


Figure 6.1-9 Scatter Graph on a Logarithmic Scale -Free Acceleration

Figure 6.1-10 shows the average for each stage for vehicle with a functional DPF(Orange dots) and a non-functional DPF(Blue dots).

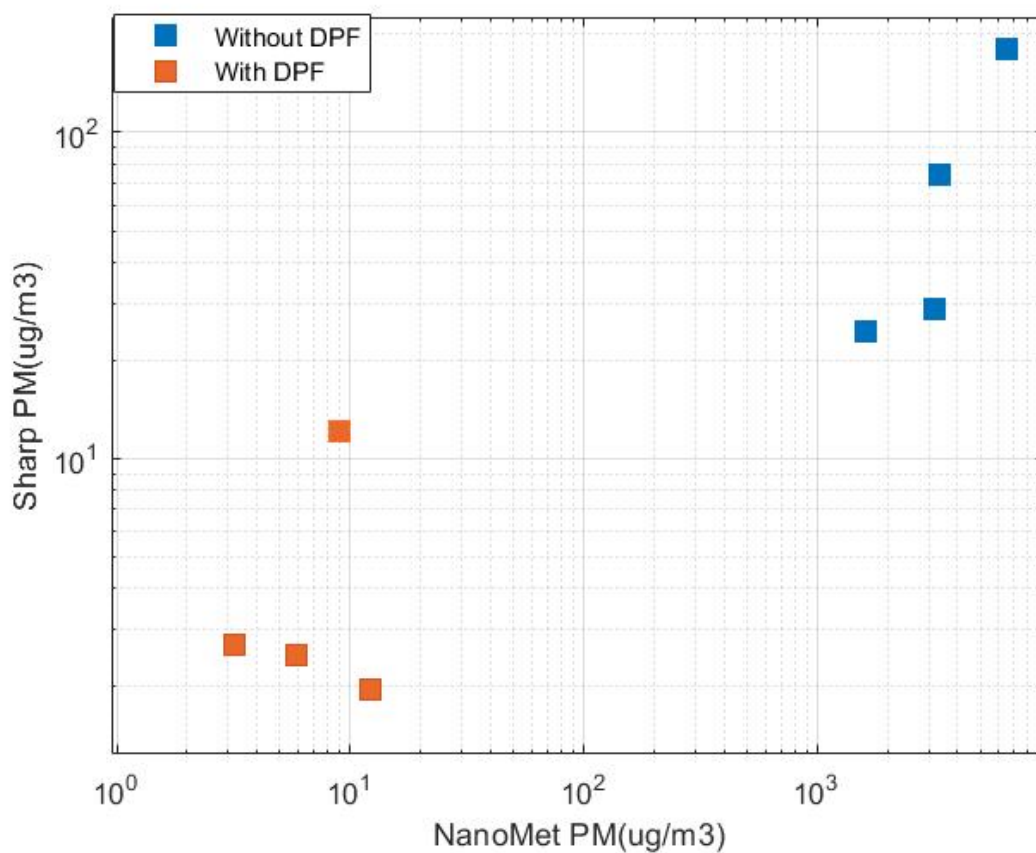


Figure 6.1-10 Scatter Graph on a Logarithmic Scale -Average from Each Stage

From the above figures, two clear zones can be seen that distinguish between a vehicle with DPF and a vehicle without DPF, noting that the observed high value of 900 $\mu\text{g}/\text{m}^3$ represents the upper end of the measurement range of the sharp sensor.

It's been observed that there is a significant difference between instruments at each stage (i.e., correlation), but the difference between the absence and presence of DPF is several orders of magnitude greater than any difference between instruments.

6.2 Future of Low-cost particle filter integrity tester

Low-cost sensors are an interesting topic in modern aerosol science due to their simplicity and availability. But it also comes with various challenges and limitations. The challenges and a possible solution are discussed below:

1. **Condensation of particles:** The SHARP sensor used in low-cost devices is based on the principle of light scattering. Particle condensation is one of the main problems with this sensor, as water absorbs radiation, and the mass concentration can be overestimated due to the reduced light intensity received by the phototransistor. Possible solutions to remedy these problems are:
 - By heating the exhaust sampling at higher temperature to prevent the condensations of an organic material
 - By flowing the sheath air to remove the condensed or dust particles from the sensing element of the sensor.
2. **Limit of detection:** The SHARP dust sensor used in low-cost device offers an easy-to-use solution at an excellent price point; however, the sensor is known to offer limited dynamic range and poor limits of detection (L.O.D.). This creates a substantial limitation, in that the sensors may only be able to be reliably used in environments where airborne particulate matter is present at high concentrations. The limit of detection can be improved by:
 - By preventing condensation of organic materials.
 - By darkening the dust sensors chamber with paint as sensor works on light scattering principle.
 - By optimizing the signal averaging.
3. **Repeatability:** The low-cost device shows moderate repeatability. The repeatability can be improved by:
 - By limiting Human error
 - By averaging the data for a longer period (i.e., Large data set).

Figure 6.2-1 shows the future low-cost device model to achieve better results. Here, instead of one sensor, three sensors are used in series with each other. The data obtained from each sensor is averaged over a period of time. Each sensor may need to be calibrated individually. HEPA filter can be used to create a sheath airflow to remove the condensed particles or dust particles from the sensor unit. The data quality of the low-cost device could be further improved by modifying the flow system and the particle concentration calculation algorithm.

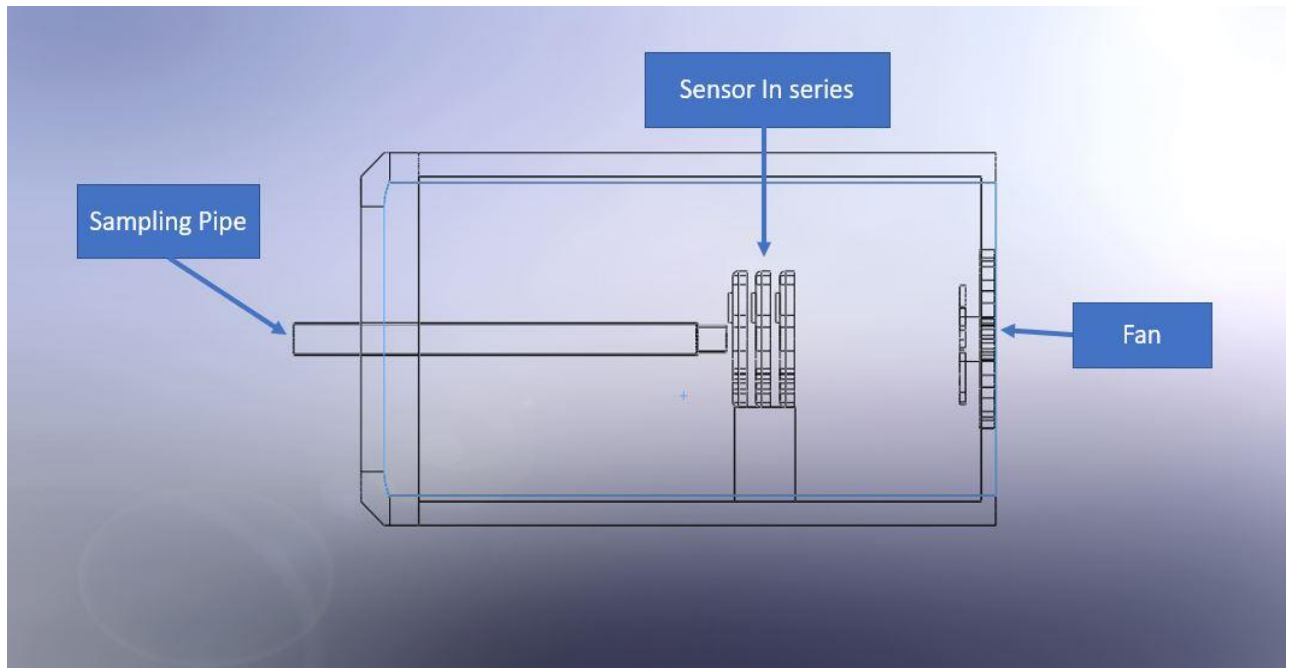


Figure 6.2-1 Future Concept Model of Low-cost Device (1)

The future model is designed to accommodate accessories such as breadboard and Arduino board in the chamber, but it should be noted that this model is only a concept that can be changed in the future according to flexibility. The expected cost of this concept model will be around 70 euros.

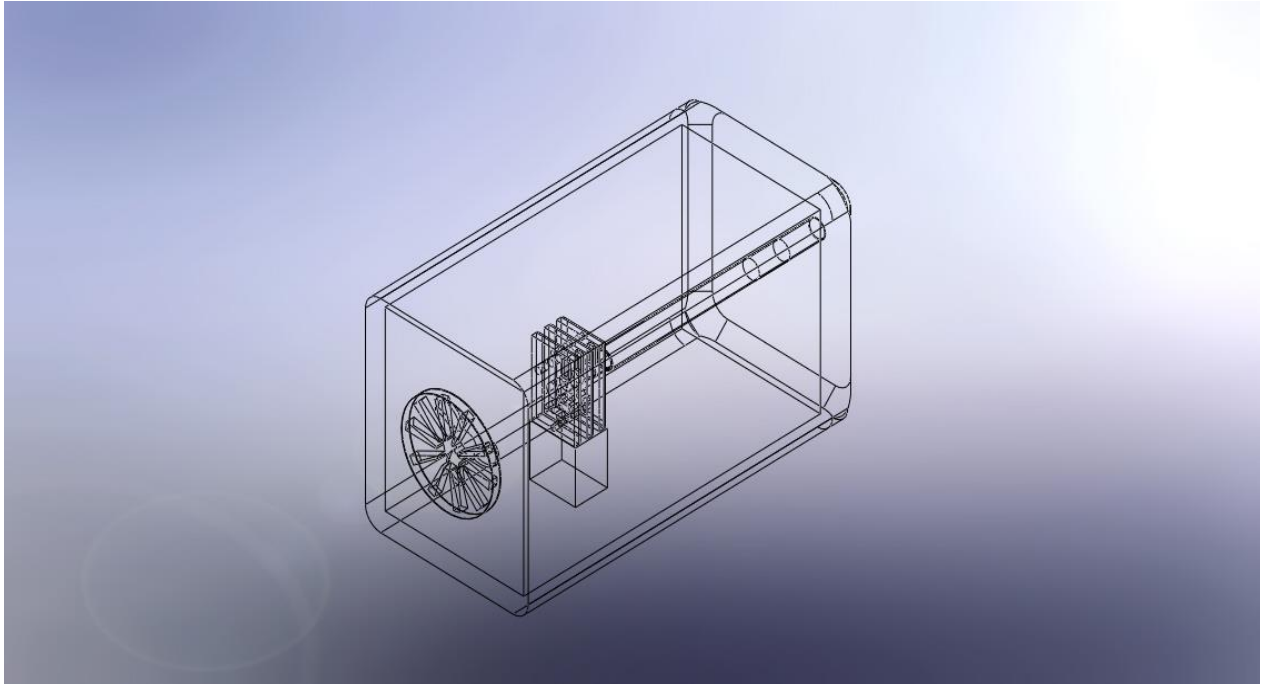


Figure 6.2-2 Future Concept Model of Low-cost Device (2)

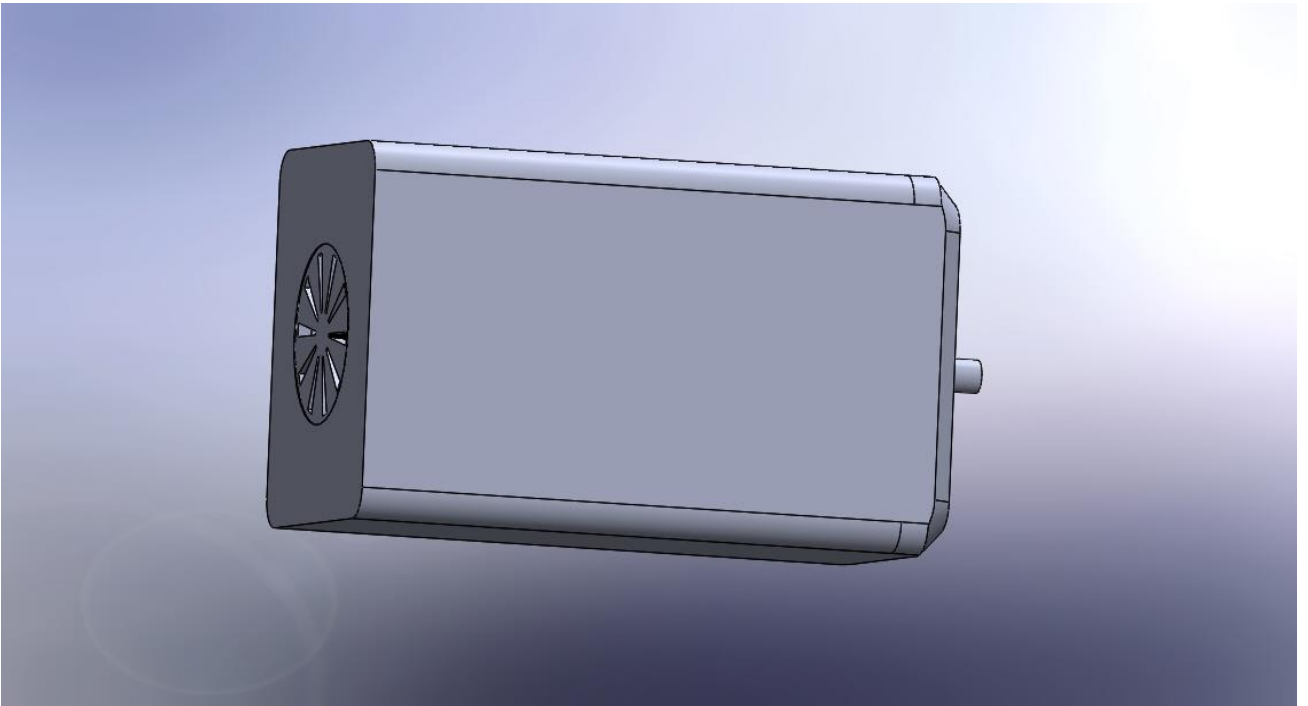


Figure 6.2-3 Future Concept Model of Low-cost Device (3)

7 Conclusion

In a pilot study conducted at Czech University of Life Sciences, various experiments were performed on the vehicles with & without DPF, and the data were analyzed by using low-cost particle filter integrity tester along with conventional high time-resolution instruments. The comparison between a low-cost device and conventional instruments were made and the ability to distinguish between a fully functioning and an absent filter on an automobile diesel engine of a low-cost device was investigated and discussed in this thesis.

Initially, the devices were synchronized in time to time-lined with each other during each stage and cycle. The particulate mass was calculated from the EEPS. The data from the low-cost device were pre-processed using the MATLAB "smoothing" command. The size distribution of the EEPS for all three vehicles was plotted to characterize the aerosol behaviour. The gain factor was used to achieve the closest match between the low-cost instrument and the standard instruments. A gain factor of 10 was used for the Roomster and a gain factor of 50 was used for the Octavia. The gain factor is based solely on observation of the curve pattern.

The repeatability of all three instruments in each phase was calculated and presented, the low-cost instrument shows moderate repeatability. The detection limit given by the manufacturer is not the same for the instrument in an open environment, so the detection limit for the low-cost instrument was determined using the approach of Kaiser and Specker. The repeatability and detection limit can be improved by following the steps described in Section 6.2

The devices were compared for each stage. From the figure, it can be seen that the low-cost instrument has the highest correlation with the standard instruments at free acceleration and at high idle. The correlation between the instruments can be improved by averaging data over a longer period of time. So, it can be concluded that the low-cost instrument is very reliable compared to other three stages at free acceleration.

In summary, the low-cost device has the potential to detect vehicles with functioning DPF and with non-functioning DPF. The summary graph was shown for the vehicle with functional DPF and non-functional DPF for the low-cost device. It was clearly observed that the vehicle without DPF has almost no concentration as compared to the vehicle with DPF. In addition, scatter plots were made showing that the efficiency of the low-cost device to distinguish between vehicles with functioning DPF and non-functioning DPF ranges from 93% to 100%. The efficiency can be improved by considering the steps described in section 6.2.

This type of low-cost device can be used in developing countries where the demand for monitoring particulate matter is particularly urgent to protect public health. The model can still be upgraded to get more accurate results and still under 100 Euros.

References

- [1] D. S. Greenbaum, "Sources of Air Pollution".
- [2] *Theory of ICE and Simulation*, Prague, 2020.
- [3] European Environment Agency, "Air quality in Europe," European Environment Agency, Luxembourg, 2020.
- [4] S. Polasa, "Comparison of Instrumentation for Online Measurement of Particle Emissions from Direct Injection Spark Ignition Engines," Prague, 2020.
- [5] *Air Pollution From Ground Transportation*, United Nations, 2002.
- [6] V. S. Petrovic, "Particulate Matter From Diesel Engine," vol. 12, pp. 183-198, 2008.
- [7] J. R. Heywood, *Internal Combustion Engine Fundamentals*, First ed., Mc Graw Hill, 1988, pp. 635-648.
- [8] S. Mohankumar and P. Senthilkumar, "Particulate matter formation and its control methodologies for diesel engine : A comprehensive review," *ELSEVIER*, pp. 1-12, 2017.
- [9] Agency, United States Environmental Protection, "Particulate Matter (PM) Pollution," [Online]. Available: <https://www.epa.gov/pm-pollution/particulate-matter-pm-basics>. [Accessed 02 06 2021].
- [10] "Ultrafine Particle Metrics and Research Considerations: Review of the 2015 UFP Workshop," *Int J Environ Res Public Health.*, vol. 13, 2016.
- [11] DieselNet, "EU: Cars and Light Trucks," [Online]. Available: <https://dieselnet.com/standards/eu/ld.php>. [Accessed 14 06 2021].
- [12] W. A. Majewski, "Diesel Particulate Filters," 2001. [Online]. Available: <http://courses.washington.edu/cive494/DPF.pdf>. [Accessed 15 06 2021].
- [13] "McCANDLESS TRUCK CENTER," [Online]. Available: <https://www.mctrux.com/--DPF-FAQs>. [Accessed 15 06 2021].
- [14] N. Hoofman, "Tampering," uCARE, 2019.
- [15] discoverdef, "discoverdef," [Online]. Available: <https://www.discoverdef.com/def-overview/selective-catalytic-reduction/>. [Accessed 03 07 2021].
- [16] "Tampering of Emission Control Systems," 2019. [Online]. Available: <https://unece.org/fileadmin/DAM/trans/doc/2019/wp29grpe/GRPE-78-04e.pdf>. [Accessed 03 07 2021].
- [17] M. Vojtišek and et.al, "Roadside Measurement of PM/PN Emissions from Individual Vehicles In

Prague," in *ETH Nanoparticle*, 2018.

- [18] Otamic, "The Irish Times," 2019. [Online]. Available: <https://www.irishtimes.com/advertising-feature/a-car-with-a-dpf-filter-removed-cannot-legally-drive-on-public-roads-in-ireland-1.4119079>. [Accessed 03 07 2021].
- [19] "DPF Delete Shop," [Online]. Available: <https://dpfdeleteshop.com>. [Accessed 03 07 2021].
- [20] "Diagnostic Anti-Tampering Systems," [Online]. Available: <https://dias-project.com/>. [Accessed 03 07 2021].
- [21] W. A. Majewski, "Emission Tampering," [Online]. Available: https://dieselnet.com/tech/emissions_tampering.php. [Accessed 03 07 2021].
- [22] M. Budde, "Distributed, Low-Cost, Non-Expert Fine Dust Sensing with Smartphones," Faculty of Informatics Karlsruhe Institute of Technology (KIT), 2018.
- [23] A. Liberti, "Modern methods for air pollution monitoring," *Pure and Applied Chemistry*, vol. 44, no. 3, pp. 519-534, 1975.
- [24] J. H. Gilliam and E. S. Hall, "Reference and Equivalent Methods Used to Measure National Ambient Air Quality Standards (NAAQS) Criteria Air Pollutants," 06 2016. [Online]. Available: https://cfpub.epa.gov/si/si_public_record_report.cfm?Lab=NERL&dirEntryId=321491. [Accessed 05 07 2021].
- [25] A. Q. E. G. (AQEG), "Methods for monitoring particulate concentrations," 2005. [Online]. Available: <https://uk-air.defra.gov.uk/assets/documents/reports/aqeg/ch5.pdf>. [Accessed 05 07 2021].
- [26] F. Doering, I. Paprotny and R. White, "MEMS Air-Microfluidic Sensor For Portable Monitoring Of Airborne Particulates," in *Solid-State Sensors, Actuators and Microsystems Workshop, Hilton Head 2012, Transducer Research Foundation, 2012*, 2012.
- [27] F. Leccese, A. Proietti and e. al., "A New Dusts Sensor for Cultural Heritage Applications Based on Image Processing," *Sensors*, vol. 14, no. 6, pp. 9813-9832, 2014.
- [28] M. Carminati, G. Ferrari and M. Sampietro, "Emerging miniaturized technologies for airborne particulate matter pervasive monitoring," *Measurement*, vol. 101, pp. 250-256, 2017.
- [29] A. Petzold and R. Niessner, "Photoacoustic soot sensor for in-situ black carbon monitoring," *Applied Physics B: Lasers and Optics*, vol. 3, no. 2, pp. 191-197, 1996.
- [30] E. Laan, D. Stam, R. Hoogeveen, G. B. CourregesLacoste and E. Boom, "'Sensitivity of the Single Particle Soot Photometer to different black carbon types," *Atmospheric Measurement Techniques*, vol. 5, no. 5, p. 1031, 2012.
- [31] DieselNet, "New Periodic Technical Inspections (NPTI)," [Online]. Available:

<https://dieselnet.com/standards/eu/pti.php>. [Accessed 05 07 2021].

- [32] W. A. Majewski and H. Jääskeläinen, "Smoke Opacity," 07 2013. [Online]. Available: https://dieselnet.com/tech/measure_opacity.php#princip. [Accessed 05 07 2021].
- [33] G. Kadijk, "PTI PN Test Procedure," 2020. [Online]. Available: <https://programacalac.com/wp-content/uploads/2019/10/9-Gerrit-Kadijk.pdf>. [Accessed 05 07 2021].
- [34] Y. Wang, J. Li, H. Jing, Q. Zhang, J. Jiang and P. Biswas, "Laboratory Evaluation and Calibration of Three Low-Cost Particle Sensors for Particulate Matter Measurement," *Aerosol Science and Technology*, pp. 1063-1077, 2015.
- [35] S. C. o. America, "Particle Sensor Model PPD42NS," 2010. [Online]. Available: https://files.seeedstudio.com/wiki/Grove_Dust_Sensor/resource/Grove_-_Dust_sensor.pdf. [Accessed 06 07 2021].
- [36] L. SAMYOUNG S&C Co., "Particle / Dust Sensor Module DSM 501 Series," 2014. [Online]. Available: <https://www.elecrow.com/download/DSM501.pdf>. [Accessed 06 07 2021].
- [37] SHARP, "GP2Y1010AU0F Compact Optical Dust Sensor," 2006. [Online]. Available: <https://pdf1.alldatasheet.com/datasheet-pdf/view/412700/SHARP/GP2Y1010AU0F.html>. [Accessed 06 07 2021].
- [38] S. T. Corp, "Application Guide for Sharp GP2Y1026AU0F Dust Sensor(Arduino Uno/Mega)," 07 2018. [Online]. Available: https://www.mouser.com/catalog/additional/Sharp_Microelectronics_Application_Guide_for_Sharp_GP2Y1026AU0F_Dust_Sensor.pdf. [Accessed 11 07 2021].
- [39] ARDUINO, "Introduction to Arduino," [Online]. Available: <https://www.arduino.cc/en/guide/introduction>. [Accessed 11 07 2021].
- [40] SHARP, "Application note of Sharp dust sensor GP2Y1010AU0F," [Online]. Available: https://global.sharp/products/device/lineup/data/pdf/datasheet/gp2y1010au_appl_e.pdf. [Accessed 11 07 2021].
- [41] S. Corporation, "GP2Y1010AU0F Compact Optical Dust Sensor," 12 2006. [Online]. Available: <https://pdf1.alldatasheet.com/datasheet-pdf/view/412700/SHARP/GP2Y1010AU0F.html>. [Accessed 11 07 2021].
- [42] T. Incorporated, "ENGINE EXHAUST PARTICLE SIZER SPECTROMETER EEPS 3090," [Online]. Available: <https://tsi.com/products/particle-sizers/particle-size-spectrometers/engine-exhaust-particle-sizer-spectrometer-eeps-3090/>. [Accessed 12 07 2021].
- [43] K. PARK, F. CAO, D. B. KITTELSON and P. H. MCMURRY, "Relationship between Particle Mass and Mobility for Diesel Exhaust Particles," *Environ. Sci. Technol*, vol. 37, pp. 577-583, 2003.
- [44] J. Olferta, J. Symonds and N. Collings, "The effective density and fractal dimension of particles emitted from a light-duty diesel vehicle with a diesel oxidation catalyst," *Aerosol Science*, pp. 69-

- [45] W. C. Hinds, *Aerosol Technology*, Wiley-Interscience, 1999.
- [46] "STUDENT", "The probable error of a mean," *Biometrika*, vol. 6, no. 1, pp. 1-25, 1908.
- [47] GitHub, "Application Guide for Sharp GP2Y1014AU0F Dust Sensor," [Online]. Available: <https://github.com/sharpsensoruser/sharp-sensor-demos/wiki/Application-Guide-for-Sharp-GP2Y1014AU0F-Dust-Sensor>. [Accessed 11 07 2021].
- [48] T. S. & C. KGaA, "testo NanoMet3 Modul for 19“ rack User manual," [Online]. Available: <https://media.testo.com/media/70/69/9f79c6aeddeb/testo-NanoMet3-Instruction-manual.pdf>. [Accessed 12 07 2021].
- [49] "Green Ship of the Future," [Online]. Available: <https://greenship.org/about/emission-wiki/particulate-matter/>. [Accessed 23 07 2021].

List of Figure

| | |
|---|----|
| Figure 1.1-1 Contribution of particle matters emission from different sources [5]..... | 5 |
| Figure 1.1-2 Stages of soot particle formation [2]..... | 6 |
| Figure 1.1-3 Particle size distribution (Where, D_p is the particle diameter, UFP are ultrafine particles, and PM stands for particulate matter.) [10]..... | 7 |
| Figure 1.1-4 Annual Concentration of PM_{10} in 2018 [3]..... | 10 |
| Figure 1.1-5 Annual Concentration of $PM_{2.5}$ In 2018 [3]..... | 11 |
| Figure 1.2-1 BASIC CONTRUCTION OF DPF..... | 14 |
| Figure 1.2-2 Particle Size Distribution of Vehicle with & without DPF [12]..... | 15 |
| Figure 1.2-3 Tampering devices shop Online [19]..... | 16 |
| Figure 1.3-1 PN Emission of Vehicle with DPF @ Low idle speed [33]..... | 20 |
| Figure 3.2-1 Sharp GP2Y1010AUOF Sensor Working Principle [38]..... | 23 |
| Figure 3.2-2 Internal working Schematic Sharp GP2Y1010AUOF [41]..... | 23 |
| Figure 3.3-1 System Connection [40]..... | 25 |
| Figure 3.3-2 Complete Circuit [46]..... | 25 |
| Figure 3.3-3 Arduino Serial Monitor Output..... | 26 |
| Figure 3.3-4 GP2Y1010AUOF Characteristics [40]..... | 26 |
| Figure 3.4-1 3D Design of Low-Cost Device..... | 27 |
| Figure 4.1-1 Unipolar Diffusion Charger [47]..... | 28 |
| Figure 4.1-2 EEPS Working Schematic [42]..... | 29 |
| Figure 4.3-1 Skoda Roomster Experiment Setup..... | 31 |
| Figure 4.4-2 Sampling Pipe of Three Instruments..... | 31 |
| Figure 4.4-3 Sampling from Tail Pipe..... | 32 |
| Figure 4.5-1 Time Synchronization Octavia(W/DPF)..... | 33 |
| Figure 4.7-1 Data Smoothing Using MATLAB..... | 34 |
| Figure 5.1-1 Particle Size Distribution IDLE..... | 36 |
| Figure 5.1-2 Particle Size Distribution IDLE 1500 rpm..... | 36 |
| Figure 5.1-3 Particle Size Distribution IDLE 2000 rpm..... | 37 |
| Figure 5.1-4 Particle Size Distribution Free Acceleration..... | 37 |
| Figure 5.2-1 High Idle Stage without Gain Factor (Octavia)..... | 38 |
| Figure 5.2-2 High Idle Stage with Gain Factor (Octavia)..... | 39 |
| Figure 5.3-1 Comparison Among Three Instruments Roomster Idle (No Load)..... | 40 |
| Figure 5.3-2 Comparison Among Three Instruments – Octavia Cold+idle..... | 40 |
| Figure 5.3-3 Comparison Among Three Instruments - Rapid (Idle)..... | 41 |
| Figure 5.3-4 High Idle (1500), No load- Roomster..... | 41 |
| Figure 5.3-5 High Idle (1500), No load - Octavia..... | 42 |
| Figure 5.3-6 High Idle (1500), No Load - Rapid..... | 42 |
| Figure 5.3-7 High Idle (2000), No Load - Roomster..... | 43 |
| Figure 5.3-8 High Idle (2000), No Load - Octavia..... | 43 |
| Figure 5.3-9 High Idle (2000), No Load - Rapid..... | 44 |
| Figure 5.3-10 Free Acceleration, No Load - Octavia..... | 44 |

| | |
|---|----|
| Figure 5.3-11 Free Acceleration, No Load - Roomster | 45 |
| Figure 5.3-12 Free Acceleration, No Load - Rapid | 45 |
| Figure 5.4-1 Repeatability of Three Instruments at Different stages (W/O DPF)..... | 46 |
| Figure 5.4-2 Repeatability of Three Instruments at shorter Interval of Free Acceleration (W/O DPF)..... | 47 |
| Figure 5.4-3 Repeatability of Three Instruments at Different stages (DPF)..... | 48 |
| Figure 6.1-1 Low-cost device at Idle | 49 |
| Figure 6.1-2 Low-cost Device at Idle 1500 RPM..... | 50 |
| Figure 6.1-3 Low-cost Device at Idle 2000 RPM..... | 50 |
| Figure 6.1-4 Low-cost Device at Free Acceleration..... | 51 |
| Figure 6.1-5 Average Values for Vehicle with & without DPF | 52 |
| Figure 6.1-6 Scatter Graph on a Logarithmic Scale - Idle..... | 53 |
| Figure 6.1-7 Scatter Graph on a Logarithmic Scale -High Idle(1500 rpm)..... | 53 |
| Figure 6.1-8 Scatter Graph on a Logarithmic Scale -High Idle (2000 rpm)..... | 54 |
| Figure 6.1-9 Scatter Graph on a Logarithmic Scale -Free Acceleration..... | 54 |
| Figure 6.1-10 Scatter Graph on a Logarithmic Scale -Average from Each Stage..... | 55 |
| Figure 6.2-1 Future Concept Model of Low-cost Device (1) | 57 |
| Figure 6.2-2 Future Concept Model of Low-cost Device (2) | 58 |
| Figure 6.2-3 Future Concept Model of Low-cost Device (3) | 58 |

List of Tables

| | |
|---|----|
| Table 1.1-1 Air quality standards by EU & WHO [3]..... | 9 |
| Table 1.1-2 emission standards for passenger cars (CI Engine) [11] | 12 |
| Table 1.1-3 EU emission standards for light commercial vehicles (CI Engine) [11]..... | 13 |
| Table 1.2-1 Comparison of PM measurement Techniques [22] | 17 |
| Table 3.2-1 Specification of Sharp GP2Y1010AUOF [38]..... | 24 |
| Table 3.5-1 Cost Estimation of Low-Cost Device | 27 |
| Table 4.3-1 Vehicle Details | 30 |

Appendix

1. Arduino Script Used During Experiment

```
////////////////////////////////////
// Sharp GP2Y1010AU0F Dust Sensor Demo
//
// Board Connection:
// GP2Y1010 Arduino
// V-LED Between R1 and C1
// LED-GND C1 and GND
// LED Pin 7
// S-GND GND
// Vo A5
// Vcc 5V
//
// Serial monitor setting:
// 9600 baud
////////////////////////////////////

// Choose program options.
#define PRINT_RAW_DATA
#define USE_AVG

// Arduino pin numbers.
const int sharpLEDPin = 7; // Arduino digital pin 7 connect to sensor LED.
const int sharpVoPin = A5; // Arduino analog pin 5 connect to sensor Vo.
const int fan = 4; // Arduino analog pin 5 connect to sensor Vo.

// For averaging last N raw voltage readings.
#ifndef USE_AVG
#define N 100
static unsigned long VoRawTotal = 0;
static int VoRawCount = 0;
#endif // USE_AVG

// Set the typical output voltage in Volts when there is zero dust.
static float Voc = 0.6;

// Use the typical sensitivity in units of V per 100ug/m3.
const float K = 0.5;

////////////////////////////////////

// Helper functions to print a data value to the serial monitor.
void printValue(String text, unsigned int value, bool isLast = false) {
  Serial.print(text);
  Serial.print("=");
  Serial.print(value);
  if (!isLast) {
```

```

    Serial.print(" ");
  }
}
void printFValue(String text, float value, String units, bool isLast = false) {
  Serial.print(text);
  Serial.print("=");
  Serial.print(value);
  Serial.print(units);
  if (!isLast) {
    Serial.print(" ");
  }
}

/////////////////////////////////////////////////////////////////

// Arduino setup function.
void setup() {
  // Set LED pin for output.
  pinMode(sharpLEDPin, OUTPUT);
  pinMode(fan, OUTPUT);

  // Start the hardware serial port for the serial monitor.
  Serial.begin(9600);

  // Wait two seconds for startup.
  delay(2000);
  Serial.println("");
  Serial.println("GP2Y1010AU0F Demo");
  Serial.println("=====");
}

// Arduino main loop.
void loop() {
  // Turn on the dust sensor LED by setting digital pin LOW.
  digitalWrite(sharpLEDPin, LOW);

  // Wait 0.28ms before taking a reading of the output voltage as per spec.
  delayMicroseconds(280);

  // Record the output voltage. This operation takes around 100 microseconds.
  int VoRaw = analogRead(sharpVoPin);

  // Turn the dust sensor LED off by setting digital pin HIGH.
  digitalWrite(sharpLEDPin, HIGH);

  // Wait for remainder of the 10ms cycle = 10000 - 280 - 100 microseconds.
  delayMicroseconds(9620);

  // Print raw voltage value (number from 0 to 1023).
  #ifndef PRINT_RAW_DATA

```

```

printValue("VoRaw", VoRaw, true);
Serial.println("");
#endif // PRINT_RAW_DATA

// Use averaging if needed.
float Vo = VoRaw;
#ifdef USE_AVG
VoRawTotal += VoRaw;
VoRawCount++;
if ( VoRawCount >= N ) {
  Vo = 1.0 * VoRawTotal / N;
  VoRawCount = 0;
  VoRawTotal = 0;
} else {
  return;
}
#endif // USE_AVG

// Compute the output voltage in Volts.
Vo = Vo / 1024.0 * 5.0;
printFValue("Vo", Vo*1000.0, "mV");

// Convert to Dust Density in units of ug/m3.
float dV = Vo - Voc;
if ( dV < 0 ) {
  dV = 0;
  Voc = Vo;
}
float dustDensity = dV / K * 100.0;
printFValue("DustDensity", dustDensity, "ug/m3", true);
Serial.println("");

  if (dustDensity>0){
    digitalWrite(fan,HIGH);
  }
  else{
    digitalWrite(fan,LOW);
  }
} // END PROGRAM

```

2. Technical data of Engine Exhaust Particle Sizer Spectrometer

| Specifications | Range |
|--|--|
| Particle size range | 5.6 to 560 nm |
| Particle size resolution | 16 channels per decade (32 total) |
| Charger mode of operation | Unipolar diffusion charger |
| Time resolution | 10 size distributions/sec |
| Flow rates Sample flow | 10 l/min |
| Sheath air | 40 l/min |
| Inlet sample temperature | 10 to 52°C |
| Operating temperature | 0 to 40°C |
| Storage temperature | -20 to 50°C |
| Atmospheric pressure correction range | 70 to 103 kPa (700 to 1034 mbar) |
| Humidity | 0 to 90% RH (noncondensing) |
| User interface | Rotary knob and display; EEPS software |
| Computer requirements | Pentium® 4 processor, 2 GHz speed or better, at least 512 MB RAM |

3. Technical data of NanoMet3

| Specifications | Range |
|---|---|
| Aerosol | Primarily diluted exhaust gases or air which contains nanoparticles |
| Concentration range | Sensor: 1E3 to 1E6 #/cm ³ . Diluted: 1E4 to 3E8 #/cm ³ |
| Particle size | 10 to 700 nm = 0.01 to 0.70 μm |
| Average particle size range (mode diameter) | 10 to 300 nm = 0.01 to 0.30 μm |
| Inlet gas flow | 4.0 l/min, actively fed to the diluter by internal pump |
| Dilution factor | Standard: 10, 100, 300; Optional one custom DF |
| Measuring gas | 1.0 l/min measuring gas |
| Power supply | 12-24 VDC, max. 60A. 90-240 VAC 50/60 Hz |
| Power consumption | nominal 650W; 300 W under standard ambient conditions |
| Evaporation tube temperatures | Ambient to 300 °C / 572 °F; accuracy ±3 °C / 5.4 °F |
| Assembly | 19" case with handles |
| Weight | approx. 18 kg; |